JOC*Article*

[^{13}C,^{15}N]2-Acetamido-2-deoxy-D-aldohexoses and Their Methyl Glycosides: Synthesis and NMR Investigations of *J*-Couplings Involving ^{1}H, ^{13}C, and ^{15}N

Yuping Zhu,[†] Qingfeng Pan,[†] Christophe Thibaudeau,[†] Shikai Zhao,[‡] Ian Carmichael,[§] and Anthony S. Serianni*,[†]

Department of Chemistry and Biochemistry and the Radiation Laboratory, University of Notre Dame, Notre Dame, Indiana 46556-5670, and Omicron Biochemicals, Inc., 1347 North Ironwood Drive, South Bend, Indiana 46615

serianni.1@nd.edu

Received July 20, 2005

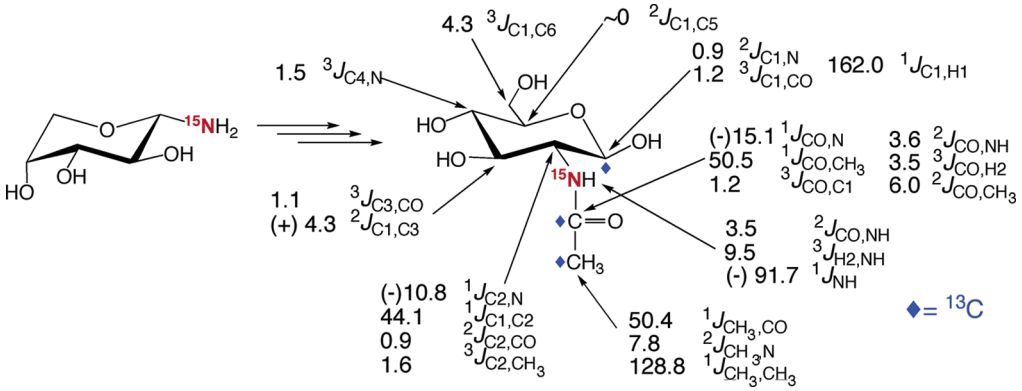

A series of 2-amino-2-deoxy-D-[1-^{13}C]aldohexoses and their methyl glycosides was prepared with use of a simplified cyanohydrin reduction route. Four D-aldopentosylamines (*arabino*, *lyxo*, *ribo*, *xylo*) were prepared from the corresponding D-aldopentoses by reaction with $NH_3(g)$ in MeOH solvent, isolated in solid form, and characterized by ^{13}C and ^{1}H NMR. Hydrolysis of β-D-xylopyranosylamine was studied using ^{13}C-labeled substrates to establish optimal solution conditions for cyanohydrin formation. Major hydrolytic intermediates were observed and identified by time-lapse 1D and 2D NMR analyses of reaction mixtures. The aldopentosylamines were subsequently employed in cyanohydrin reduction reactions with K^{13}CN to yield C2-epimeric [1-^{13}C]2-aminosugars, which were separated by chromatography on ion-exchange columns. *N*-Acetylation and methyl glycosidation followed by chromatography gave pure 2-acetamido-2-deoxy-D-[1-^{13}C]aldohexopyranosides. J_{CH} and J_{CC} spin−spin coupling constants involving the labeled anomeric carbon were measured and compared to those observed previously in methyl D-[1-^{13}C]-aldohexopyranosides. In parallel studies, theoretical *J*-couplings were calculated in model *N*-acetylated aldopyranosides using density functional theory (DFT) to predict the effect of OH vs $NHCOCH_3$ substitution at C2 on J_{CH} and J_{CC} values in aldopyranosyl rings. The synthetic method was also modified to accommodate ^{15}N- and ^{13}C-labeling within the *N*-acetyl side-chain, and some *J*-couplings involving ^{1}H, ^{13}C, and ^{15}N atoms in 2-[1,2-$^{13}C_2$;^{15}N]acetamido-2-deoxy-D-[1-^{13}C]glucose were measured and interpreted.

Introduction

2-Aminosugars are common constituents of biologically important oligosaccharides appended to glycoproteins and glycolipids.[1] For example, the core pentasaccharide (**1**) of *N*-linked glycoproteins such as human IgG contains two α-Man*p*, one β-Man*p*, and two β-GlcNAc*p* residues, with one of the latter attached covalently to Asn of the protein.[2] Structure **1** is

* Address correspondence to this author.
[†] Department of Chemistry and Biochemistry, University of Notre Dame.
[‡] Omicron Biochemicals, Inc.
[§] Radiation Laboratory, University of Notre Dame.

(1) Allen, H. J.; Kisailus, E. C. *Glycoconjugates*: *Composition, Structure and Function*; MarcelDekker: New York, 1992.

10.1021/jo051510k CCC: $33.50
Published on Web 12/15/2005

SCHEME 1

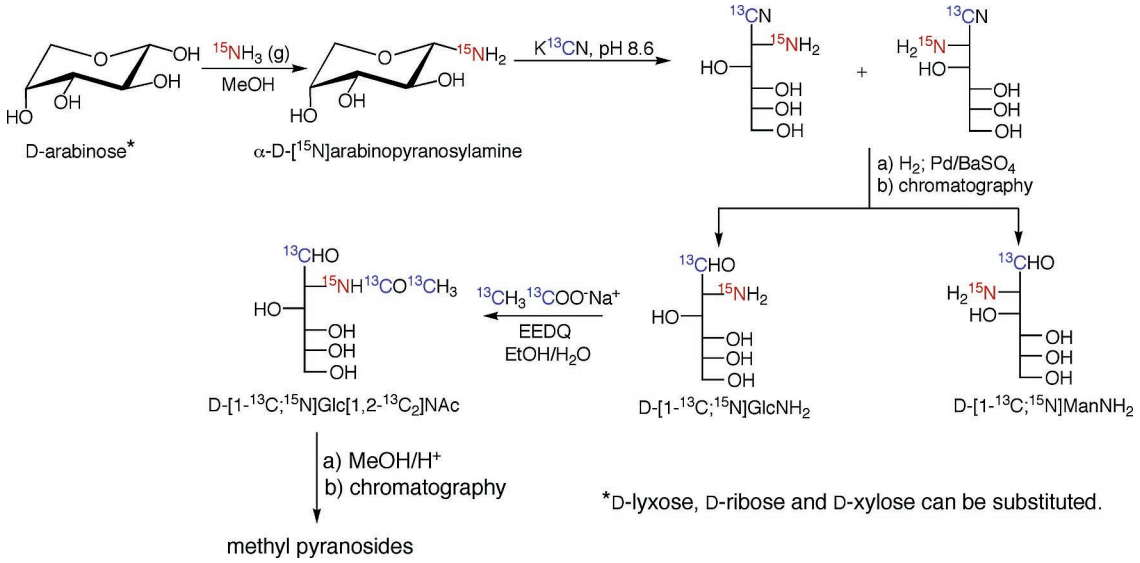

subsequently decorated in vivo with D-galactose, D-mannose, L-fucose, and/or sialic acid. Ongoing structural studies of **1**, and

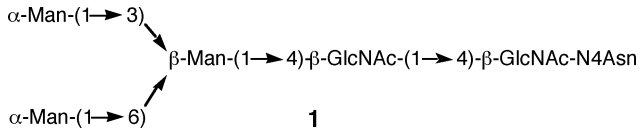

compounds derived from it, involve the use of multiple NMR parameters such as trans-glycoside *J*-couplings[3a−c] ($^2J_{CC}$, $^3J_{CC}$, and $^3J_{CH}$), dipolar[3d−g] and quadrupolar[4] couplings ($^1D_{CC}$, $^1D_{CH}$, ^{2}H QCC) and spin relaxation to investigate their conformations and dynamics in solution. These studies are facilitated by isotopic labeling with ^{13}C, ^{2}H, and/or ^{15}N at one or more sites.[5]

Synthetic methods are available to prepare a wide range of D-mannose and D-galactose ^{13}C isotopomers,[6] and sialic acid labeled at C1, C2, and/or C3 is prepared enzymically from unlabeled ManNAc and labeled pyruvate using sialic acid aldolase.[7] However, current methods[8] to label GlcNAc, and to label sialic acid at C4−C9 using labeled ManNAc, are not sufficiently simple, general, and/or reliable for routine use in isotope labeling of oligosaccharides. In this report, a simple and general chemical route to 2-amino-2-deoxy-D-aldohexoses is described that allows site-specific labeling with ^{13}C and/or ^{2}H at virtually any carbon or hydrogen, and also supports ^{15}N labeling of the side-chain (Scheme 1). Using this approach, 2-amino-2-deoxy-D-[1-^{13}C]aldohexoses and their 2-acetamido-2-deoxy methyl glycopyranosides were prepared, and NMR and computational (density functional theory; DFT) studies were conducted to extend current knowledge of the structural dependencies of *J*-couplings involving ^{1}H, ^{13}C, and/or ^{15}N in aminosugars.

Experimental Section

A. General Procedure for the Synthesis of D-Aldopentopyranosylamines 2−5 (Scheme 1).[9a] Absolute MeOH (6 mL) was added to a 250 mL Erlenmeyer flask, and the flask was sealed with a rubber septum, weighed, and cooled to 4 °C in an ice bath. The cooled solution was aerated with NH_3 gas for ∼3 min and weighed to determine the amount of dissolved gas (∼1.2 g, ∼71 mmol). Dry, finely powdered D-arabinose, D-lyxose, D-ribose, or D-xylose (Sigma) (5.0 g, 33.3 mmol) was added and the flask was sealed with a rubber septum. After gentle swirling, the pentose slowly dissolved, yielding a straw-colored solution after ∼15 min. The sealed reaction vessel was allowed to stand at room temperature for 2 days, yielding crystals of the *lyxo*-**3**, *ribo*-**4**, and *xylo*-**5** glycosylamines (Scheme 2). The crystals were removed, washed with three 5-mL volumes of absolute MeOH, and dried. Isolated yields ranged from 66% to 95%. For D-arabinosylamine **2**, the reaction solution was concentrated in vacuo, yielding a crude solid determined by NMR to be >95% pure (Figure 1); unreacted D-arabinose was the contaminant.

Compounds **2**−**5** were characterized by ^{1}H and ^{13}C NMR by dissolving them in 0.1 M Na phosphate buffer at pD 10.5. Under these conditions, hydrolysis rates were very low and spectral characteristics allowed complete analyses (Figure 1).

B. General Procedure for the Synthesis of ^{13}C-Labeled 2-Amino-2-deoxy-D-[1-^{13}C]aldohexoses. In a well-vented hood,

(2) (a) Fujii, S.; Nishiura, T.; Nishikawa, A.; Miura, R.; Taniguchi, N. *J. Biol. Chem.* **1990**, *265*. (b) Dwek, R. A.; Lellouch, A. C.; Wormald, M. R. *J. Anat.* **1995**, *187*, 279−292. (c) Wormald, M. R.; Rudd, P. M.; Harvey, D. J.; Chang, S.-C.; Scragg, I. G.; Dwek, R. A. *Biochemistry* **1997**, *36*, 1370−1380.

(3) (a) Bose, B.; Zhao, S.; Stenutz, R.; Cloran, F.; Bondo, P. B.; Bondo, G.; Hertz, B.; Carmichael, I.; Serianni, A. S. *J. Am. Chem. Soc.* **1998**, *120*, 11158−11173. (b) Cloran, F.; Carmichael, I.; Serianni, A. S. *J. Am. Chem. Soc.* **1999**, *42*, 9843−9851. (c) Cloran, F.; Carmichael, I.; Serianni, A. S. *J. Am. Chem. Soc.* **2000**, *122*, 396−397. (d) Tian, F.; Al-Hashimi, H. M.; Craighead, J. L.; Prestegard, J. H. *J. Am. Chem. Soc.* **2001**, *123*, 485−492. (e) Yi, X.; Venot, A.; Glushka, J.; Prestegard, J. H. *J. Am. Chem. Soc.* **2004**, *126*, 13636−13638. (f) Martin-Pastor, M.; Bush, C. A. *Biochemistry* **2000**, *39*, 4674−4683. (g) Kiddle, G. R.; Homans, S. W. *FEBS Lett.* **1998**, *436*, 128−130.

(4) (a) Homans, S. W.; Kjellberg, A. *J. Magn. Reson.* **2001**, *151*, 90−93. (b) Bose-Basu, B.; Zajicek, J.; Bondo, G.; Zhao, S.; Kubsch, M.; Carmichael, I.; Serianni, A. S. *J. Magn. Reson.* **2000**, *144*, 207−216.

(5) Milton, M. J.; Harris, R.; Probert, M. A.; Field, R. A.; Homans, S. W. *Glycobiology* **1998**, *8*, 147−153.

(6) Serianni, A. S.; Vuorinen, T.; Bondo, P. *J. Carbohydr. Chem.* **1990**, *9*, 513−541.

(7) (a) Augé, C.; David, S.; Gautheron, C.; Malleron, A.; Cavayé, B. *New J. Chem.* **1988**, *12*, 733−744. (b) Fitz, W.; Schwark, J.-R.; Wong, C.-H. *J. Org. Chem.* **1995**, *60*, 3663−3670.

(8) Walker, T. E.; Barker, R. *Carbohydr. Res.* **1978**, *64*, 266−270.

(9) (a) This procedure differs from that reported previously (Isbell, H. S.; Frush, H. L. *J. Org. Chem.* **1958**, *23*, 1309−1319) in that only NH_3(g) is used to effect the conversion of aldose to glycosylamine. (b) Vogel, A. I. *Elementary Practical Organic Chemistry*; John Wiley and Sons: New York, 1958; pp 758−759.

SCHEME 2. Preferred Anomeric Configurations and Ring Conformation of D-Aldopentosylamines 2−5 in Aqueous Solution Observed after Dissolution of Solid Samples

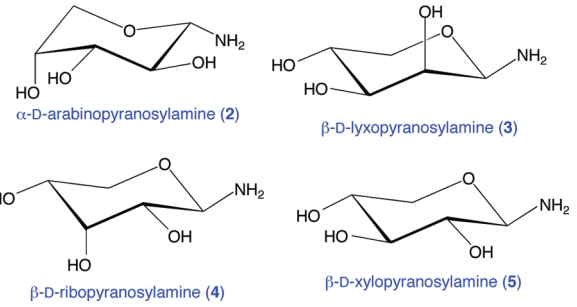

K^{13}CN (99 atom % ^{13}C; Cambridge Isotope Laboratories, Inc.) (4.0 g, 60 mmol) was dissolved in 15 mL of water in a 25 mL flask, a pH electrode was inserted, and the solution was stirred gently with a magnetic stirrer. The solution pH was adjusted to 8.6 with the *slow* addition of glacial acetic acid (∼2 mL), followed by batchwise addition of the D-aldopentosylamine (3.0 g, 20.1 mmol). After amine addition, the pH was immediately readjusted to pH 8.6 with acetic acid, and the reaction was allowed to proceed at room temperature for ∼6 min while maintaining the pH at 8.6. The pH was then lowered to 4.2 with acetic acid, and the resulting solution was purged with N_2 through a methanolic-KOH trap to remove excess H^{13}CN.[6]

Pd/$BaSO_4$ catalyst (5%; Aldrich) (1.0 g) was suspended in a minimal volume of H_2O and prereduced at atmospheric pressure over an H_2 atmosphere at room temperature, using a custom-made catalytic reduction apparatus.[9b] The HCN-purged reaction mixture was then added, and aldononitrile reduction was initiated. H_2 gas consumption was monitored via gas displacement in a water ballast, and the reaction was terminated when consumption ceased (∼18 mmol of H_2 was consumed; 3−5 h). The suspension was filtered to remove the catalyst (glass-fiber filter), and the filtrate was concentrated at 30 °C in vacuo to a minimal volume to obtain the crude C2-epimeric aminosugars (∼3.5 g).

The crude aminosugar solution was applied to a column (5.0 cm i.d. × 53 cm) containing Dowex 50 × 8 (200−400 mesh) ion-exchange resin in the H^+ form.[8] The column was eluted with a 4 L linear HCl gradient (0−0.5 M) at a flow rate of ∼1.2 mL/min. Fractions (∼20 mL) were assayed by spotting aliquots (3 μL) from each fraction onto a Whatman filter paper, drying, and spraying with a ninhydrin reagent (0.2 g of ninhydrin in 70 mL of absolute ethanol, 2 mL of H_2O, and 8 mL of pyridine; amine-containing spots appear purple after heating). A broad band of aminosugar eluted between fractions 267 and 307. In the $GlcNH_2$/$ManNH_2$ synthesis, the *gluco* product predominated (∼80%), and the elution profile revealed some overlap between the two products, with the *gluco* epimer eluting first. Careful pooling of fractions gave pure samples of each amine: from 20.1 mmol of **2**, $GlcNH_3Cl$, 0.49 g, 2.3 mmol; $ManNH_3Cl$, 0.15 g, 0.7 mmol; mixture, 0.83 g, 3.8 mmol, total yield, 34%. In the $GalNH_2$/$TalNH_2$ synthesis, *galacto* eluted first, followed by *talo*, with some overlap: from 33.5 mmol of **3**, $GalNH_3Cl$, 1.4 g (6.5 mmol), $TalNH_3Cl$, 1.5 g (7.0 mmol), total yield, 62% (6.2 g). For the $GulNH_2$/$IdoNH_2$ synthesis, *gulo* eluted first, followed by *ido*, with some overlap: from 35.8 mmol of **5**, $GulNH_3Cl$, 1.0 g (4.6 mmol); $IdoNH_3Cl$, 1.0 g (4.6 mmol), total yield, 63% (4.9 g). Pooled fractions were concentrated at 30 °C in vacuo to dryness to yield a crude solid.

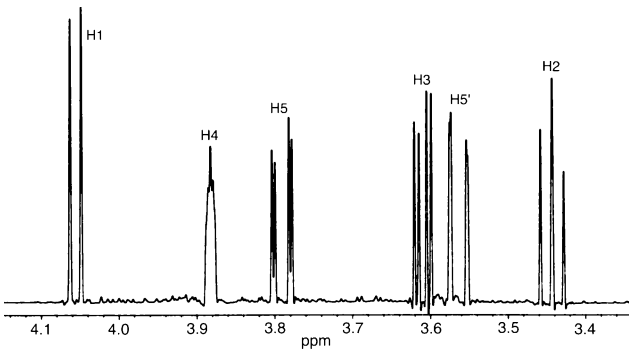

FIGURE 1. ^{1}H NMR spectrum (600 MHz) of D-arabinopyranosylamine (**2**) in aqueous (^2H_2O) solution at pD 10.5 (0.1 M Na phosphate buffer) and 20 °C, showing signal assignments. At this pH, sample stability is high and spectral resolution sufficient to permit the measurement of *J*-couplings; significant line broadening is observed under neutral and acidic pH values, where hydrolysis is more rapid.

C. General Procedure for *N*-Acetylation. 2-Amino-2-deoxy-D-aldohexose hydrochloride (0.15 g, 0.6 mmol) was dissolved in a minimal volume of H_2O, and the solution pH was adjusted to 6.6 with use of Dowex 1 × 8 (200−400 mesh) (OH^-) anion-exchange resin. The resin was removed by filtration and washed, the filtrates were combined (total volume of ∼6 mL), and EtOH (25 mL) was added. Potassium acetate (0.1 g, 1 mmol, dissolved in a small amount of H_2O) and EEDQ (2-ethoxy-1-ethoxycarbonyl-1,2-dihydroquinone) (0.18 g, 0.7 mmol dissolved in 10 mL of EtOH) were added to the aminosugar solution with stirring. The reaction vessel was sealed with a rubber septum, covered with aluminum foil, and allowed to stand at 30 °C for 24 h. Reaction progress was monitored by TLC (ethyl acetate:pyridine:H_2O, 10:4:3): R_f 0.31 (free amine), R_f 0.71 (*N*-acetyl derivative).

After the reaction was complete, the reaction mixture was evaporated from 20 mL of H_2O to remove ethanol. EEDQ was extracted with 6 × 15 mL volumes of CH_2Cl_2, and the resulting aqueous solution was deionized with batchwise additions of excess Dowex 50 × 8 (20−50 mesh) (H^+) and Dowex 1 × 8 (20−50 mesh) (OAc^-) ion-exchange resins. The deionized solution was concentrated at 30 °C in vacuo to remove acetic acid, and the solid residue was crystallized from water/MeOH. *N*-Acetylation yields ranged from 45% to 80%. The crude *N*-acetylated aminosugars were glycosidated without further purification.

D. General Procedure for Methyl Glycosidation. 2-Acetamido-2-deoxy-D-aldohexose (0.19 g, 0.85 mmol) was dissolved in 20 mL of absolute MeOH, and Dowex HCR−W2 (H^+) resin[10] was added with gentle stirring. The reaction mixture was refluxed for 1 h then filtered, and the filtrate was concentrated to give crude glycoside (∼0.2 g, 0.85 mmol). The product was dissolved in a minimal volume of H_2O and loaded on a column (2.5 cm i.d. × 105 cm) containing Dowex 1 × 8 (200−400 mesh) (OH^-) ion-exchange resin.[11a] The column was eluted with distilled H_2O (1.5 mL/min), and fractions testing positive for aminosugar (phenol−H_2SO_4 assay)[11b] were pooled and concentrated at 30 °C in vacuo. For the *gluco* isomer, the α-pyranoside **7** eluted first (60 mg, 0.25 mmol, 29%), followed by the *β*-pyranoside **8** (65 mg, 0.28 mmol, 33%). Yields were comparable for the other glycosidation reactions. Eight methyl 2-acetamido-2-deoxy-D-[1-^{13}C]aldopyranosides **6**−**13** were prepared (Scheme 3). For *galacto* and *talo* configurations, only one product (α-pyranosides **6** and **13**) was isolated by chromatography. For the *gulo* and *manno* configurations, the α-pyranoside eluted first, followed by the *β*-pyranoside.

E. General Procedure for ^{15}N-Labeling. The synthetic procedure described for ^{13}C-labeling (see above) was followed, but substituting $^{15}NH_3(g)$ for unlabeled $NH_3(g)$ in the protocol. $^{15}NH_3(g)$ from a small low-pressure gas cylinder (Cambridge Isotope Laboratories, Inc.) was *slowly* bubbled into the cold methanol solvent held in a tared flask. After ∼1 min, the gas flow was stopped and the reaction vessel weighed to determine the weight of the dissolved

(10) Podlasek, C. A.; Wu, J.; Stripe, W. A.; Bondo, P. B.; Serianni, A. S. *J. Am. Chem. Soc.* **1995**, *117*, 8635−8644.

(11) (a) Austin, P. W.; Hardy, F. E.; Buchanan, J. C.; Baddiley, J. *J. Chem. Soc.* **1963**, 5350−5353. (b) Hodge, J. E.; Hofreiter, B. T. *Methods Carbohydr. Chem.* **1962**, *1*, 380−394.

SCHEME 3

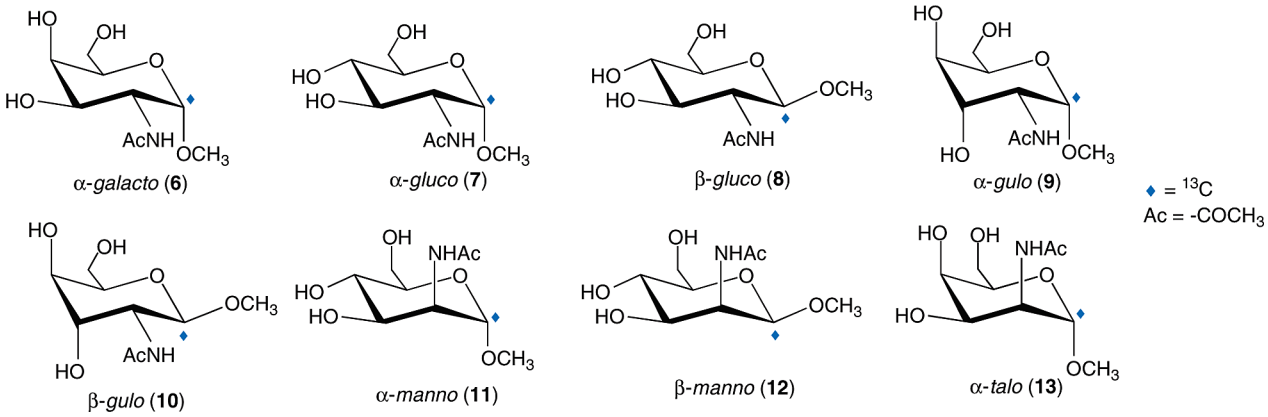

gas. The process was repeated if necessary. A 4-fold molar excess of $^{15}NH_3(g)$ was found to be sufficient to convert the pentoses almost completely into glycosylamines. In the present work, no effort was made to recover $^{15}NH_3(g)$ lost to the atmosphere, although this could be achieved by passing the released gas through an aqueous HCl trap.

F. Mass Spectrometry. Mass spectra (FAB mode) of [1-^{13}C]-**6**−**13** were obtained on a JEOL JMS-AX505HA mass spectrometer with 3-nitrobenzyl alcohol as the solvent. All spectra showed $(M + 1)^+$ ions at *m*/*z* 237 and $(M + Na)^+$ ions at *m*/*z* 259 (Figure S1, Supporting Information). Fragmentation ions were also observed at *m*/*z* 205 (M − 31) and *m*/*z* 187 (M − 49) presumably caused by the loss of OCH_3 and $OCH_3 + H_2O$, respectively. HRMS data for the aldopentosylamines **2**−**5** are given in Table S1 (Supporting Information). Exact masses are provided for both the monomeric and dimeric forms of these amines, each of which are detected by MS analysis (see the Supporting Information for the structure of the dimer).

G. NMR Spectroscopy. 1D ^{1}H and ^{13}C{^{1}H} NMR spectra were obtained in ^2H_2O on a Varian Unity*Plus* 600 MHz FT-NMR spectrometer. Samples were analyzed in 3 mm NMR tubes with a Nalorac dual ^{13}C/^{1}H microprobe. ^{13}C Signal assignments for **6**−**13** were made via 2D HMQC spectra[12] and interpretation of J_{CC} values observed in [1-^{13}C] derivatives. $^2J_{C1,H2}$ coupling signs were determined from analyses of relative cross-peak displacements in ^{1}H−^{1}H TOCSY spectra[13a,b] of [1-^{13}C] derivatives.

^{1}H−^{1}H and ^{13}C−^{1}H NMR spin−spin coupling constants (*J*-couplings) in **6**−**13** were determined by simulation of ^{1}H spectra with MacNUTs (Acorn NMR) (Figure S2, Supporting Information).[14] Couplings are reported in hertz and are accurate to within ±0.1 Hz unless otherwise indicated.

H. High-Pressure Liquid Chromatography. HPLC was performed on a ternary HPLC pump connected to an RI detector. The RI detector was interfaced with desktop PC running ChromPerfect HPLC software (Justice Laboratory Software, Version 5.1.0) for data processing. A Rezex RCM (Ca^{2+}) monosaccharide column (7.8 × 300 mm; Phenomenex) contained in a column heater equipped with a heater controller was equilibrated at 85 °C, using deionized/degassed water as the solvent. Solvent flow rate was set at 0.6 mL/min, and sample retention times were recorded in minutes using the ChromPerfect software.

I. Mechanistic Studies of β-D-Xylopyranosylamine Hydrolysis. β-D-[1-^{13}C]- and [5-^{13}C]Xylopyranosylamines were prepared from D-[1-^{13}C]xylose and D-[5-^{13}C]Xylose, respectively. D-[1-^{13}C]Xylose was prepared from D-threose and K^{13}CN as described previously.[6,15] D-[5-^{13}C]Xylose was prepared from D-[6-^{13}C]glucose.[16] The latter compound was converted to 1,2-*O*-isopropylidene-α-D-[6-^{13}C]-glucofuranose,[17] which was treated consecutively with $Pb(OAc)_4$, $NaBH_4$, and aqueous HCl to give D-[5-^{13}C]xylose after purification by chromatography on Dowex 50 × 8 (200−400 mesh)(Ca^{2+}).[18a] Treatment of D-[5-^{13}C]xylose with $NaMoO_4$[18b] gave D-[5-^{13}C]lyxose, which was converted to [5-^{13}C]**3** and used to determine preferred anomeric configuration in solution (see below).

For NMR studies of amine hydrolysis, reactions were conducted at pH 6.5−8.5 for defined time periods, and then quenched by raising the solution pH to ∼10.5 with NaOH. At pH 10.5, hydrolysis rates were low enough to permit the characterization of reaction intermediates by 2D NMR where more extended acquisition times were required. Characterization of the intermediates observed during β-D-xylopyranosylamine hydrolysis was assisted by the use of 2D HMQC[12] and HMQC-TOCSY[19] spectra and D-[1-^{13}C]- and [5-^{13}C]-xylopyranosylamines as substrates.

Computations

A. Geometry Optimizations. Ab initio molecular orbital calculations (geometric optimizations and *J*-coupling calculations) were conducted with use of *Gaussian*98.[20] For geometry optimization, density functional theory (DFT) was employed with the B3LYP functional[21] and the 6-31G* basis set[22] (B3LYP/6-31G*).

(12) Bax, A.; Subramanian, S. *J. Magn. Reson.* **1986**, *67*, 565−569.
(13) (a) Wijmenga, S. S.; Hallenga, K.; Hilbers, C. W. *J. Magn. Reson.* **1989**, *84*, 634−642. (b) Serianni, A. S.; Podlasaek, C. A. *Carbohydr. Res.* **1994**, *259*, 277−282.
(14) *MacNUTs Pro*; Acorn NMR, Inc.: Livermore, CA.
(15) Serianni, A. S.; Nunez, H. A.; Barker *Carbohydr. Res.* **1979**, *72*, 71−78.
(16) King-Morris, M. J.; Bondo, P. B.; Mrowca, R. A.; Serianni, A. S. *Carbohydr. Res.* **1988**, *175*, 49−58.
(17) Schmidt, O. T. In *Methods in Carbohydrate Chemistry*; Whistler, R. L., Wolfrom, M. L., Eds.; Academic Press: New York, 1963; Vol. 2, pp 318−325.
(18) (a) Angyal, S. J.; Bethell, G. S.; Beveridge, R. *Carbohydr. Res.* **1979**, *73*, 9−18. (b) Hayes, M. L.; Pennings, N. J.; Serianni, A. S.; Barker, R. *J. Am. Chem. Soc.* **1982**, *104*, 6764−6769.
(19) Wijmenga, S. S.; Hallenga, K.; Hilbers, C. W. *J. Magn. Reson.* **1989**, *84*, 634−642.
(20) Frisch, M. J.; Trucks, G. W.; Schlegel, H. B.; Scuseria, G. E.; Robb, M. A.; Cheeseman, J. R.; Zakrzewski, V. G.; Montgomery, J. A., Jr.; Stratmann, R. E.; Burant, J. C.; Dapprich, S.; Millam, J. M.; Daniels, A. D.; Kudin, K. N.; Strain, M. C.; Farkas, O.; Tomasi, J.; Barone, V.; Cossi, M.; Cammi, R.; Mennucci, B.; Pomelli, C.; Adamo, C.; Clifford, S.; Ochterski, J.; Petersson, G. A.; Ayala, P. Y.; Cui, Q.; Morokuma, K.; Malick, D. K.; Rabuck, A. D.; Raghavachari, K.; Foresman, J. B.; Cioslowski, J.; Ortiz, J. V.; Baboul, A. G.; Stefanov, B. B.; Liu, G.; Liashenko, A.; Piskorz, P.; Komaromi, I.; Gomperts, R.; Martin, R. L.; Fox, D. J.; Keith, T.; Al-Laham, M. A.; Peng, C. Y.; Nanayakkara, A.; Challacombe, M.; Gill, P. M. W.; Johnson, B.; Chen, W.; Wong, M. W.; Andres, J. L.; Gonzalez, C.; Head-Gordon, M.; Replogle, E. S.; Pople, J. A. *Gaussian98*, Revision A.9; Gaussian, Inc.: Pittsburgh, PA, 1998.
(21) Becke, A. D. *J. Chem. Phys.* **1993**, *98*, 5648−5652.
(22) Hehre, W. J.; Ditchfield, R.; Pople, J. A. *J. Chem. Phys.* **1972**, *56*, 2257−2261.

SCHEME 4

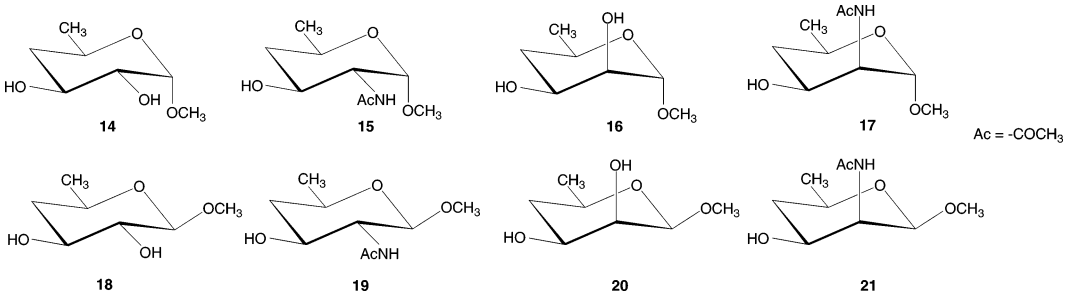

B. *J*-Coupling Calculations. NMR *J*-couplings were calculated by DFT using a modified version of *Gaussian*94[23] and an extended basis set[24] ([5s2p1d|3s1p]) designed to recover the Fermi contact contribution to the coupling. Actual calculated couplings are reported (i.e., the reported values were not scaled). Given the relatively small magnitudes of ^2J and ^3J, absolute errors are estimated to be ±0.4 Hz.

Eight model compounds **14**−**21** were chosen for the computations that mimic the methyl glycosides of α-Glc (**14**), α-GlcNAc (**15**), α-Man (**16**), α-ManNAc (**17**), β-Glc (**18**), β-GlcNAc (**19**), β-Man (**20**), and β-ManNAc (**21**) (Scheme 4). These structures lack OH substituents at C4 and C6. Initial exocyclic torsions used for geometry optimization were as follows: C2−C1−O1−CH_3, 180°; C1−C2−O2−O2H, 180°; C2−C3−O3−O3H, 180°; H2−C2−N2−N2H, 180°. In all calculations, the amide configuration was trans (amide hydrogen trans to amide oxygen).

Results and Discussion

A. Synthesis of ^{13}C-Labeled Aminosugars. The route shown in Scheme 1 is a modification of a previous synthetic approach used to prepare D-[1-^{13}C]GlcNH_2 and D-[1-^{13}C]ManNH_2 from *N*-benzyl-D-arabinosylamine and K^{13}CN.[8] The new route has significant advantages over the prior approach. Simple glycosylamines are employed that are easily prepared on a large scale and in good yield, and are obtainable in crystalline or amorphous solid forms. These amines exhibit good chemical stability if stored in a dry container at 4 °C. Introduction of ^{15}N is also simplified (see below), requiring relatively inexpensive $^{15}NH_3$ gas rather than ^{15}*N*-benzylamine as the isotope source reagent. Cyanohydrin reduction yielded two C2-epimeric 2-aminoaldoses, in some cases with one isomer highly favored (e.g., $GlcNH_2$/$ManNH_2$, ∼3/1). These products were separated as the free amines by chromatography on Dowex 50 × 8 (200−400 mesh) (H^+) ion-exchange resin. Alternatively, the amine mixture can be *N*-acetylated, and the resulting 2-acetamido epimers separated by chromatography on Dowex 50 × 8 (200−400 mesh) (Ca^{2+}) ion-exchange resin analogous to the analytical scale separations (Table S1, Supporting Information; see below). In this work, three of the four aldopentosylamines (**2**, **3**, and **5**) were used as cyanohydrin substrates; amine **4** is expected to behave similarly.

Conversion of the ^{13}C-labeled *N*-acetylated aminosugars to their methyl pyranosides by Fischer glycosidation proceeded rapidly and in good yield. Separation of the anomeric mixtures was achieved by chromatography on Dowex 1 × 8 (200−400 mesh) (OH^-) ion-exchange resin, and the purified products were analyzed by HPLC (Table S2, Supporting Information). Retention times varied from ∼11.5−14.1 min, with the *galacto* configuration considerably more retained. HPLC of the reducing sugars showed progressively increasing retention times in the series ManNAc, GlcNAc, and GalNAc, in agreement with the glycoside results (Table S2, Supporting Information). Interestingly, HPLC of Man, Glc, and Gal showed Glc eluting first, followed by the nearly coeluting Man and Gal, indicating that the *N*-acetyl group modulates binding interactions on the column and thus affects the elution order.

TABLE 1. ^{1}H[a] and ^{13}C[b] Chemical Shifts, and ^{1}H-^{1}H Spin-Coupling Constants,[c] in D-Aldopentopyranosylamines 2−5 in ^2H_2O (pD 10.5; 0.1 M Na Phosphate Buffer)

	aldopentosylamine ring configuration			
	arabino-**2**	*lyxo*-**3**	*ribo*-**4**	*xylo*-**5**
δ_{H1}	4.056	4.235	4.383	3.990
δ_{H2}	3.446	3.828	3.415	3.103
δ_{H3}	3.610	3.526	4.093	3.378
δ_{H4}	3.884	3.741	3.780	3.561
δ_{H5}	3.793	3.845	3.678	3.851
$\delta_{H5'}$	3.566	3.168	3.540	3.252
δ_{C1}	90.24	86.02	86.15	88.54
δ_{C2}	72.95	73.73	72.38	76.83
δ_{C3}	75.75	76.47	72.60	79.26
δ_{C4}	71.29	68.92	69.53	72.13
δ_{C5}	69.63	68.97	65.87	68.92
$^3J_{H1,H2}$	8.6	1.1	8.4	8.7 (7.8)[e]
$^3J_{H2,H3}$	9.5 (10.1)[d]	3.4	2.9	9.1 (9.3)
$^3J_{H3,H4}$	3.5 (3.5)	9.7	2.9	9.2 (9.1)
$^3J_{H4,H5}$	2.3 (1.5)	5.5	4.9	5.4 (5.5)
$^3J_{H4,H5'}$	1.4 (2.1)	10.6	10.1	10.8 (10.5)
$^2J_{H5,H5'}$	−13.0 (−12.8)	−11.3	−11.2	−11.4 (−11.6)
$^3J_{C5,H1}$		1.2		

[a] In ppm, ±0.001 ppm relative to internal 3-(trimethylsilyl)-1-propanesulfonic acid, 20 °C. [b] In ppm, ±0.01 ppm; ^{13}C signal assignments were determined from 2D ^{13}C−^{1}H HMQC spectra. [c] In Hz, ±0.1 Hz. [d] Values in parentheses are couplings observed in methyl β-D-arabinopyranoside (ref 10). [e] Values in parentheses are couplings observed in methyl β-D-xylopyranoside (ref 10).

B. D-Aldopentosylamine Conformation. Studies of hydrolysis rates of D-xylopyranosylamine at different solution pH values revealed good stability at alkaline pH (e.g., pD 10.5). ^{13}C{^{1}H} and ^{1}H NMR spectra of **2**−**5** were obtained under these conditions, yielding high-resolution spectra (Figure 1, Table 1). The D-aldopentosylamines crystallize/solidify as pyranoses (initially demonstrated by obtaining ^{1}H NMR spectra of **2**−**5** in anhydrous DMSO-d_6 solvent; data not shown). On the basis of ^{1}H−^{1}H spin-coupling analysis in ^2H_2O solutions at pD 10.5 (0.1 M Na phosphate buffer) (Table 1), the D-*lyxo*-**3**, D-*ribo*-**4**, and D-*xylo*-**5** configurations crystallize in the $^4C_1$ ring conforma-

(23) Frisch, M. J.; Trucks, G. W.; Schlegel, H. B.; Gill, P. M. W.; Johnson, B. G.; Robb, M. A.; Cheeseman, J. R.; Keith, T.; Petersson, G. A.; Montgomery, J. A.; Raghavachari, K.; AlLaham, M. A.; Zakrzewski, V. G.; Ortiz, J. V.; Foresman, J. B.; Peng, C. Y.; Ayala, P. Y.; Chen, W.; Wong, M. W.; Andres, J. L.; Replogle, E. S.; Gomperts, R.; Martin, R. L.; Fox, D. J.; Binkley, J. S.; Defrees, D. J.; Baker, J.; Stewart, J. P.; Head Gordon, M.; Gonzalez, C.; Pople, J. A. *Gaussian94*, Gaussian, Inc.: Pittsburgh, PA, 1995.

(24) Stenutz, R.; Carmichael, I.; Widmalm, G.; Serianni, A. S. *J. Org. Chem.* **2002**, *67*, 949−958.

SCHEME 5

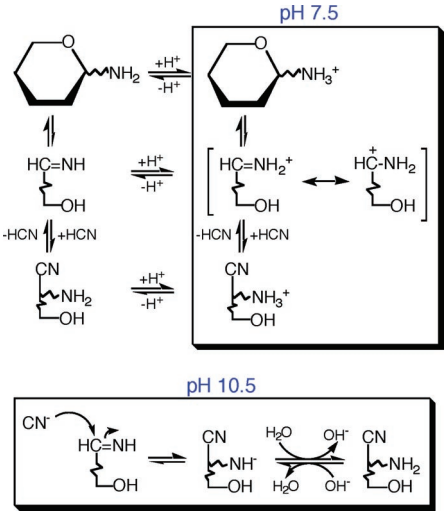

tion, whereas D-*arabino*-**2** prefers the $^1C_4$ form (Scheme 2). Anomeric configurations in the crystalline (or amorphous solid) state were determined from $^3J_{H1,H2}$ values observed in aqueous solution at pD 10.5 in **2** (8.6 Hz; α-pyranose), **4** (8.4 Hz; *β*-pyranose), and **5** (8.7 Hz; *β*-pyranose) (Scheme 2). For **3**, $^3J_{H1,H2}$ could not be used reliably because the coupling is small in both anomers. In this case, the assignment was made by measuring $^3J_{C5,H1}$ in [5-^{13}C]**3**; the observed coupling (1.2 Hz) confirmed the *β*-configuration (a coupling >5 Hz is expected in the α-anomer).[25a]

The favored pyranosyl ring conformations of **2**−**5** orient the C1−N1 bond equatorial in aqueous solution at pD 10.5. For **2** and **5**, preferred anomeric configurations and ring conformations are identical to those observed in the D-aldopentopyranoses[25a] and methyl D-pentopyranosides.[10] For **3** and **4**, replacement of OH with NH_2 at C1 enhances the stability of the $^4C_1$ form (i.e., *β*-D-lyxopyranose is ∼87% $^4C_1$ and *β*-D-ribopyranose is ∼74% $^4C_1$,[25a] whereas $^4C_1$ is almost exclusively favored by the corresponding glycosylamines). For **3**, the favored anomer shifts from α in the reducing sugar ($^1C_4$ (∼38%) and $^4C_1$ (∼62%))[25a] to *β* (almost exclusively $^4C_1$) in the glycosylamine. These observations suggest that preferred anomeric configuration[25b] and ring conformation in **2**−**5** are correlated and influenced strongly by the orientational requirements of the C1−N1 bond.

C. D-Xylopyranosylamine Hydrolysis. Solution conditions for cyanide addition to **2**−**5** significantly affect the overall yield of aminosugar. Cyanide addition under mildly basic conditions (pH 7.5) probably occurs via the acyclic protonated imine, which is a more potent electrophile than the unprotonated imine that predominates at higher pH (pH 10.5) (Scheme 5). At higher pH, cyanohydrin hydrolysis rates increase,[25c] which reduces the aminosugar yield. At the same time, pH 7.5 favors the protonated HCN (pK_a = 9.2), which is less nucleophilic than

SCHEME 6

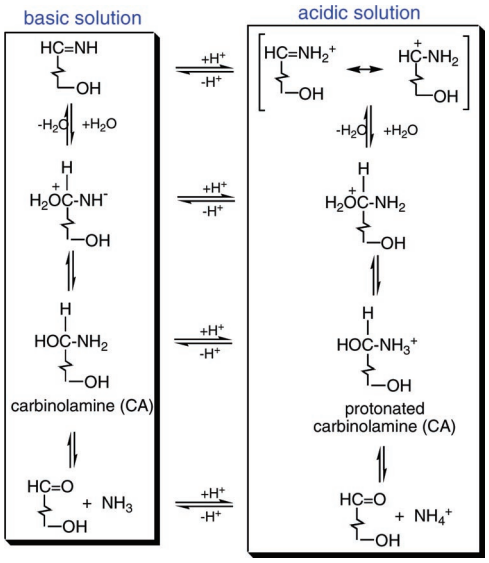

CN^- predominating at pH 10.5 (Scheme 5). Competing with cyanide addition is glycosylamine hydrolysis (Scheme 6). Hydrolysis rates are much greater at pH 7.5 than at pH 10.5, presumably because the protonated imine is more prone to attack by water. Optimal pH conditions were examined that promote cyanide addition while reducing glycosylamine and aldononitrile hydrolysis, and pH 8.5 was found to be optimal. At this pH, cyanide addition was rapid and essentially irreversible, and minimal (<10%) hydrolysis was observed.

^{13}C NMR studies were conducted to monitor the hydrolysis of *β*-D-[1-^{13}C]xylopyranosylamine **5** under different solution conditions. At pH 10.5, hydrolysis was slow, but anomerization to α-D-[1-^{13}C]xylopyranosylamine was observed early in the reaction, followed by the slow appearance of putative xylofuranosylamines (data not shown). At alkaline pH, anomerization between xylopyranosylamine anomers appears to be more kinetically favored than pyranosylamine−furanosylamine and furanosylamine−furanosylamine anomerization.

A typical time-lapse $^{13}C\{^1H\}$ NMR spectrum of a *β*-D-[1-^{13}C]xylopyranosylamine hydrolysis reaction mixture after ∼10 min at pH 6.5 showed ^{13}C signals arising primarily from seven labeled species (Figure 2). Three of these signals were assigned to *β*-D-[1-^{13}C]xylopyranosylamine (*βp*A) ($^1J_{C1,H1}$ = 154.3 Hz; $^3J_{H1,H2}$ = 8.8 Hz), α-D-[1-^{13}C]xylopyranose (α*p*) ($^1J_{C1,H1}$ = 169.5 Hz; $^3J_{H1,H2}$ = 3.7 Hz), and *β*-D-[1-^{13}C]-xylopyranose (*βp*) ($^1J_{C1,H1}$ = 161.5 Hz; $^3J_{H1,H2}$ = 7.9 Hz) based on known C1 chemical shifts[26] and $^1J_{C1,H1}$.[27] The HMQC spectrum (Figure 3) obtained without ^{13}C-decoupling yielded characteristic ^{1}H chemical shifts for these three species. HMQC-TOCSY spectra (Figure 4) extended the proton correlations beyond H1, confirming the assignments. The ^{13}C signal at 81.03 ppm (Figure 2) was assigned to α-D-[1-^{13}C]xylopyranosylamine (α*p*A) based on $^3J_{H1,H2}$ (∼3 Hz) and $^1J_{C1,H1}$ (∼158 Hz), and on its rate of formation during the reaction. The α/*β* ratio of D-xylopyranosylamines observed throughout the course of hydrolysis was considerably smaller than that observed for

(25) (a) Wu, J.; Bondo, P. B.; Vuorinen, T.; Serianni, A. S. *J. Am. Chem. Soc*. **1992**, *114*, 3499−3505. (b) This argument rests on the assumption that anomeric equilibrium has been reached in aqueous solutions of the aldopentopyranosylamines at pD 10.5. In contrast to aldopentoses where equilibration rates are relatively rapid, anomerization rates of the glycosylamines at this pH are considerably slower. However, hydrolysis mechanism studies of **5** at pH 6.5 (see text) where anomerization rates are more rapid showed a greater *β*-pyranose/α-pyranose ratio compared to that observed in free xylose, supporting the conclusion that the stability of the equatorial C1−N1 bond is enhanced in the amines. (c) Serianni, A. S.; Nunez, H. A.; Barker, R. *J. Org. Chem*. **1980**, *45*, 3329−3341.

(26) Bock, K.; Pedersen, C. *Adv. Carbohydr. Chem. Biochem*. **1983**, *41*, 27−66.

(27) Drew, K. N.; Zajicek, J.; Bondo, G.; Bose, B.; Serianni, A. S. *Carbohydr. Res*. **1998**, *307*, 199−209.

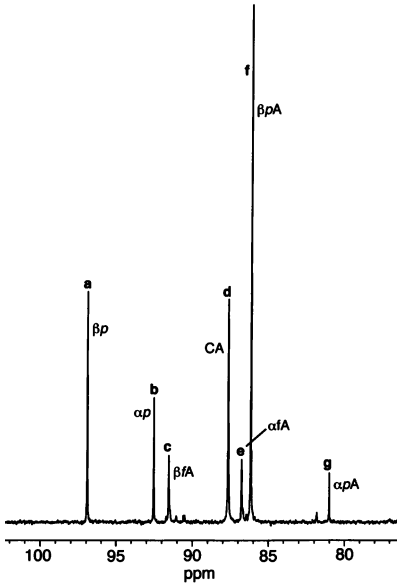

FIGURE 2. ^{13}C NMR spectrum at 20 °C of a β-D-[1-^{13}C]xylopyranosylamine hydrolysis reaction mixture (pH 6.5, ~10 min reaction time). Seven enriched signals are detected in the anomeric region: β-D-[1-^{13}C]xylopyranose (96.94 ppm, βp), α-D-[1-^{13}C]xylopyranose (92.53 ppm, αp), β-D-[1-^{13}C]xylofuranosylamine (91.55 ppm, βfA), acyclic [1-^{13}C]carbinolamine (87.66 ppm, CA), α-D-[1-^{13}C]xylofuranosylamine (86.77 ppm, αfA), β-D-[1-^{13}C]xylopyranosylamine (86.18 ppm, βpA), and α-D-[1-^{13}C]xylopyranosylamine (81.03 ppm, αpA). The small signals near 82 and 90 ppm were not identified.

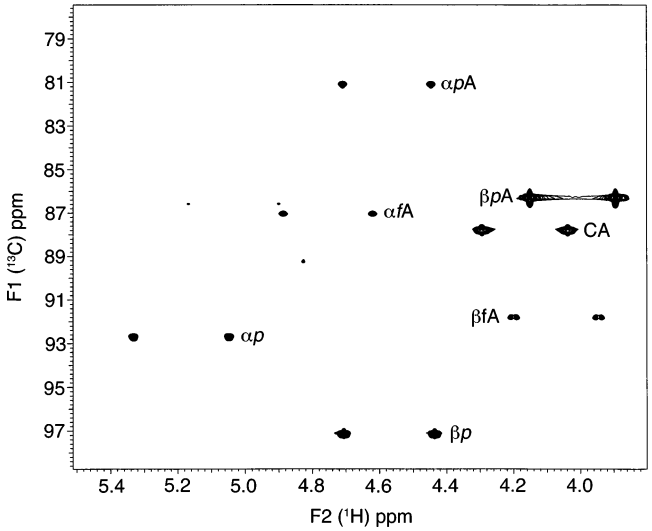

FIGURE 3. 2D ^{13}C−^{1}H HMQC spectrum (^{13}C-coupled) at 20 °C of the reaction mixture described in Figure 2. Data were used to assign the H1 resonances of each form, each of which appears as paired signals in the ^{1}H dimension due to $^{1}J_{CH}$. These assignments were used to determine $^{3}J_{H1,H2}$ and $^{1}J_{C1,H1}$ values (see text) from the ^{1}H NMR spectrum of the same mixture (data not shown).

D-xylopyranoses,[27] reflecting the increased preference for an equatorial orientation of the C1−N1 bond in the amines (see above).

The three remaining signals in Figure 2 were assigned by using NMR and reaction kinetics data. Two of these signals at 91.55 ($^{1}J_{C1,H1}$ = 153.1 Hz) and 86.77 ppm ($^{1}J_{C1,H1}$ = ~160 Hz) were assigned to β-D-xylofuranosylamine (βfA) and α-D-xylofuranosylamine (αfA), respectively. These assignments were based partly on HMQC-TOCSY data obtained on D-[5-^{13}C]-

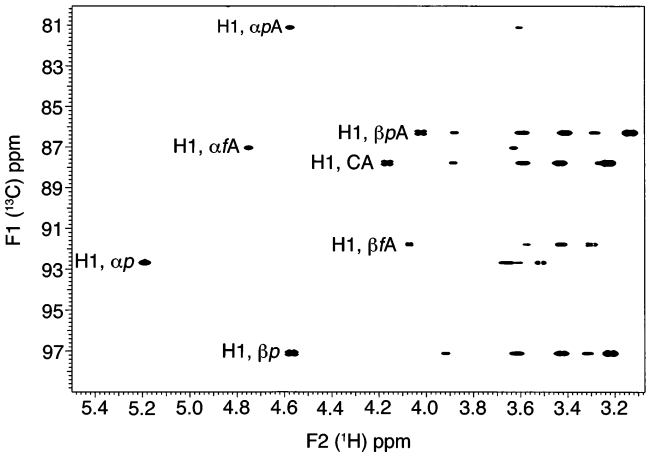

FIGURE 4. 2D ^{13}C−^{1}H HMQC-TOCSY spectrum at 20 °C of the reaction mixture described in Figure 2 (60 ms mixing time). Note the significant TOCSY transfer for βpA, CA, βfA, and βp, which contain large $^{3}J_{H1,H2}$ values. In contrast, TOCSY correlations for αpA, αfA, and αp are more limited due to inefficient magnetization transfer from H1 and H2 in these forms ($^{3}J_{H1,H2}$ is small).

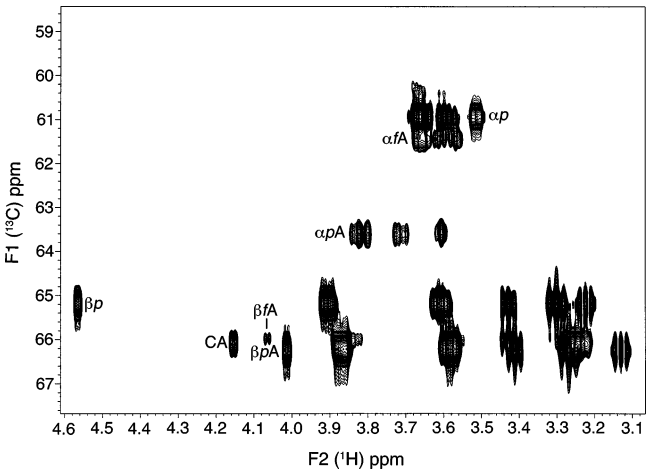

FIGURE 5. 2D ^{13}C−^{1}H HMQC-TOCSY spectrum at 25 °C of a reaction mixture obtained from the hydrolysis of β-D-[5-^{13}C]xylopyranosylamine (pH 6.5; 80 ms mixing time). Note the significantly different C5 chemical shifts for the D-xylofuranosylamines (αfA, ~61 ppm; βfA, ~66 ppm); similar differences have been observed for xylofuranoses.[28] Note also the detection of H1 for βp, CA, βpA, and βfA (i.e., completeTOCSY transfer through the structure), whereas H1 (andother) correlations are absent for αpA, αfA, and αp.

xylopyranosylamine hydrolysis (Figure 5). These data, and those from the HMQC-TOCSY spectrum (Figure 4), revealed C5 chemical shifts for these species at 61.2 (α) and 65.8 ppm (β), values consistent with exocyclic hydroxymethyl carbons of xylofuranosyl anomers.[28]Assignment of the two C1 signals to specific furanose anomers was based on the reported effect of *cis*-1,2 electronegative substituents on C1 chemical shifts in furanoses; the *trans*-N1,O2 anomer (β) is expected to yield a C1 signal downfield of the *cis*-N1,O2 anomer (α).[29,30]

The remaining signal at 87.66 ppm in Figure 2 was assigned to the acyclic carbinolamine (CA), a presumed hydrolytic

(28) Snyder, J. R.; Serianni, A. S. *Carbohydr. Res.* **1987**, *163*, 169−188.
(29) Ritchie, R. G. S.; Cyr, N.; Korsch, B.; Koch, H. J.; Perlin, A. S. *Can. J. Chem.* **1975**, *53*, 1424−1433.
(30) Serianni, A. S.; Barker, R. *J. Org. Chem.* **1984**, *49*, 3292−3300.

SCHEME 7

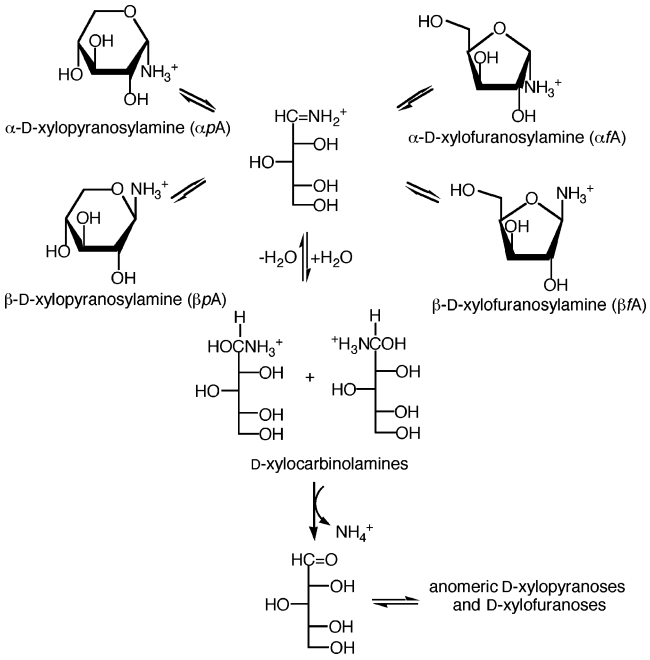

intermediate (Scheme 6). Formation of the acyclic carbinolamine is rapid and its steady-state concentration remains relatively high during the course of hydrolysis. An overall reaction scheme for *β*-D-xylopyranosylamine hydrolysis at pH 6.5 is summarized in Scheme 7.

Several interesting structural observations emerged from these hydrolysis studies. The H1 signal of the acyclic xylocarbinolamine (CA) appears as a doublet at ∼4.15 ppm with a $^{3}J_{H1,H2}$ value of 8.8 Hz. When the same species contains ^{13}C-enrichment at C1, however, the H1 signal appears as a pseudoquartet split by the directly bonded ^{13}C. These results suggest that, in the absence of ^{13}C-enrichment, the C1-epimeric carbinolamines have identical δ_{H1}. Upon ^{13}C-enrichment, however, this degeneracy is eliminated due to different $^{1}J_{C1,H1}$ values in the two diastereomers (150 and 158 Hz).

$^{3}J_{H1,H2}$ values in the D-xylofuranosylamines also deserve comment. In the α-configuration, $^{3}J_{H1,H2}$ = 3.3 Hz, which is similar to $^{3}J_{H1,H2}$ values observed in 5-deoxy-α-D-xylofuranose (3.9 Hz) and 5-*O*-methyl-α-D-xylofuranose (4.3 Hz).[28] In contrast, $^{3}J_{H1,H2}$ in *β*-D-xylofuranosylamine (8.8 Hz) is significantly larger than that observed in 5-deoxy-*β*-D-xylofuranose (1.7 Hz) and 5-*O*-methyl-*β*-D-xylofuranose (1.4 Hz), suggesting a major change in conformational preference. The strong equatorial preference of the C1−N1 bond observed in **2**−**5** may explain these observations. C1−N1 bond orientation dictates ring conformation in xylofuranosylamines, in both cases leading to preferred furanose conformations that orient this bond quasi-equatorial. In the α-furanose, this conformation is near E_2, whereas in the *β*-furanose it is near ^{2}E (Scheme 8). In the xylofuranoses, the C1−O1 bond prefers a quasi-axial orientation due to the anomeric effect (Scheme 8).[30] Thus, $^{3}J_{H1,H2}$ will not change significantly when O1 is substituted by NH_2 in the α-*xylo* configuration, since the H1−C1−C2−H2 torsion angle remains approximately gauche in both structures. In contrast, this torsion angle changes from gauche to trans in the *β*-*xylo* configuration, causing a significant increase in $^{3}J_{H1,H2}$. The unusually large $^{3}J_{H1,H2}$ in *β*-D-xylofuranosylamine suggests that pseudorotation is more restricted in this structure compared to *β*-D-xylofuranose,

SCHEME 8

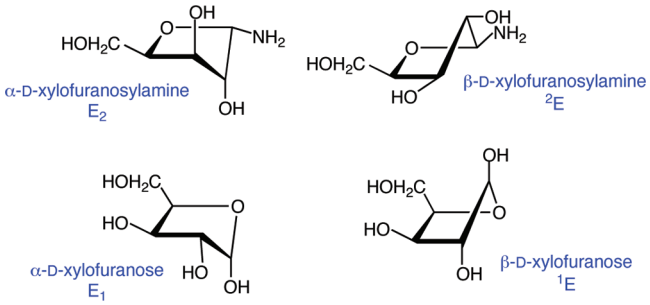

and the same may be true for α-D-xylofuranosylamine. These conclusions are consistent with conformational predictions reported recently for aldofuranosylamines based on DFT calculations.[31]

D. ^{1}H and ^{13}C NMR Analyses of 6−13. ^{1}H and ^{13}C chemical shifts and J_{HH}, J_{CH}, and J_{CC} values in **6**−**13** are reported in Tables 2−6. Substitution of an $NHCOCH_3$ for an OH substituent at C2 uniformly shifts δ_{H2} downfield by 0.2−0.4 ppm; the magnitude of the effect appears to depend on relative configuration at C1 and C2 (Table 2). The same substitution shifts δ_{C2} *upfield* by ∼18 ppm; in this case, the effect of relative configuration at C1 and C2 appears smaller (Table 3). In both cases, however, a relatively wide range of chemical shifts is observed: for δ_{H2}, 3.7−4.5 ppm and for δ_{C2}, 47−56 ppm, depending on the configuration of the pyranosyl ring. Resonances for the amide carbonyl carbons were observed at ∼175 ppm.

$^{3}J_{HH}$ values in **6**−**13** are similar to those observed in the corresponding methyl aldohexopyranosides in most cases, although $^{3}J_{H2,H3}$ is uniformly larger in the aminosugars by 0.7−1.6 Hz (Table 4). The latter change is attributed mainly to local electronegative substituent effects on the coupling rather than to conformational change, since the adjacent $^{3}J_{HH}$ are less affected, especially $^{3}J_{H3,H4}$. Couplings involving the hydroxymethyl protons of **12** also differ from those in methyl *β*-D-mannopyranoside, suggesting possible differences in C5−C6 bond rotamer populations. Long-range (4-bond) ^{1}H−^{1}H couplings were observed between H1 and H3, and between H2 and H4, in nearly all of the aminosugars studied (Table 4); the presence of these couplings and their negative signs were confirmed via spectral simulation. $^{4}J_{H2,H4}$ is especially large in **13** (−1.2 Hz) in which the di-equatorial orientation of the coupled protons creates a planar W-shaped arrangement along the coupling pathway;[32] similar couplings have been observed previously in talopyranoses.[33]

$^{1}J_{C1,H1}$ values show the expected dependence on anomeric configuration, with axial C1−H1 bonds (*β*-pyranoses) yielding smaller couplings by ∼10 Hz than equatorial C1−H1 bonds (α-pyranoses) (Table 5).[34] These couplings increase by 0.5−2.7 Hz in the aminosugars compared to related values in the corresponding methyl aldohexopyranosides. Interestingly,

(31) Cloran, F.; Zhu, Y.; Osborn, J.; Carmichael, I.; Serianni, A. S. *J. Am. Chem. Soc.* **2000**, *122*, 6435−6448.
(32) Barfield, M.; Dean, A. M.; Fallick, C. J.; Spear, R. J.; Sternwell, S.; Westerman, P. W. *J. Am. Chem. Soc.* **1975**, *97*, 1482−1492.
(33) Snyder, J. R.; Johnston, E. R.; Serianni, A. S. *J. Am. Chem. Soc.* **1989**, *111*, 2681−2687.
(34) (a) Bock, K.; Lundt, I.; Pedersen, C. *Tetrahedron Lett.* **1973**, 1037−1040. (b) Bock, K.; Pedersen, C. *J. Chem. Soc., Perkin Trans. 2* **1974**, 293−297. (c) Bock, K.; Pedersen, C. *Acta Chem. Scand.* **1975**, *B29*, 258−264.

TABLE 2. ^{1}H Chemical Shifts[a] in Methyl 2-Acetamido-2-deoxy-D-[1-^{13}C]Aldohexopyranosides

	^{1}H chemical shift (ppm)								
compd	H1	H2	H3	H4	H5	H6	H6′	OCH_3	CH_3
α-GalNAc **6**	4.824	4.197	3.910	4.015	3.953	3.813	3.790	3.419	2.075
	4.935	*3.917*	*3.906*	*4.063*	*3.997*	*3.855*	*3.832*	*3.511*	
α-GlcNAc **7**	4.787	3.943	3.741	3.508	3.700	3.907	3.811	3.415	2.067
	4.904	*3.655*	*3.761*	*3.495*	*3.741*	*3.965*	*3.852*	*3.515*	
β-GlcNAc **8**	4.494	3.738	3.584	3.488	3.510	3.987	3.801	3.557	2.088
	4.472	*3.358*	*3.588*	*3.477*	*3.560*	*4.024*	*3.822*	*3.670*	
α-GulNAc **9**	4.819	4.302	3.924	3.860	4.157	3.816	3.801	3.435	2.095
β-ManNAc **12**	4.719	4.511	3.831	3.542	3.433	3.943	3.842	3.533	2.082
	4.658	*4.072*	*3.721*	*3.652*	*3.459*	*4.021*	*3.825*	*3.630*	
α-TalNAc **13**	4.776	4.151	4.064	4.011	3.919	3.852	3.797	3.430	2.075
	4.969	*3.943*	*3.933*	*4.009*	*3.973*	*3.933*	*3.869*	*3.519*	

[a] In ^2H_2O at 25 °C; ppm (±0.001 ppm) relative to the residual ^1H_2O signal (4.800 ppm); determined by spectral simulation. Values in italics are for the corresponding methyl aldopyranosides (ref 10).

TABLE 3. ^{13}C Chemical Shifts[a] in Methyl 2-Acetamido-2-deoxy-D-[1-^{13}C]Aldohexopyranosides

	^{13}C chemical shift (ppm)								
compd	C1	C2	C3	C4	C5	C6	OMe	CO	Me_{Ac}
α-GalNAc **6**	99.09	50.80	68.73b	69.43b	71.66	62.21	56.03	175.53	22.87
	[99.1]	[50.8]	[68.7]	[69.4]	[71.6]	[62.1]	*56.0*		
	100.1	*69.2*	*70.5*	*70.2*	*71.6*	*62.2*			
α-GlcNAc **7**	98.51	54.05	71.57	70.41	72.09	61.01	55.56	174.87	22.33
	[98.6]	[54.3]	[71.9]	[70.4]	[72.2]	[61.4]	[55.6]		
	100.0	*72.2*	*74.1*	*70.6*	*72.5*	*61.6*	*55.9*		
β-GlcNAc **8**	102.36	55.88	74.40	70.38	76.32	61.18	57.49	175.10	22.60
	[102.3]	[56.1]	[74.6]	[70.9]	[76.3]	[61.5]	[57.2]		
	104.0	*74.1*	*76.8*	*70.6*	*76.8*	*61.8*	*58.1*		
α-GulNAc **9**	99.05	47.24	69.82b	69.52b	67.19	62.19	56.37	174.94	22.79
	100.4	*65.5*	*71.4*	*70.4*	*67.3*	*62.0*	*56.3*		
β-GulNAc **10**	100.96	51.00	69.29[b]	70.87[b]	74.88	61.95	57.64	175.02	22.87
	102.6	*69.1*	*72.3*	*70.5*	*74.9*	*62.1*	*58.1*		
α-ManNAc **11**	100.33	52.90	69.52[b]	67.08[b]	72.58	60.78	55.19	175.21	22.33
	101.9	*71.2*	*71.8*	*68.0*	*73.7*	*62.1*	*55.9*		
β-ManNAc **12**	100.43	53.02	72.02	66.75	76.42	60.39	57.00		21.99
	101.3	*70.6*	*73.3*	*67.1*	*76.6*	*61.4*	*56.9*		
α-TalNAc **13**	100.21	51.61	63.85	68.48	71.16	61.57	54.88	174.28	22.49
	102.2	*70.7*	*66.2*	*70.3*	*72.1*	*62.3*	*55.6*		

[a] In ^2H_2O at 25 °C; ppm (±0.01 ppm) relative to the C1 signal of α-D-[1-^{13}C]mannopyranose (95.5 ppm). Values in brackets were taken from ref 26. Values in italics are for the corresponding methyl aldopyranosides (ref 26). [b] Assignments may be reversed.

TABLE 4. ^{1}H−^{1}H Spin-Coupling Constants[a] in Methyl 2-Acetamido-2-deoxy-D-[1-^{13}C]Aldohexopyranosides

	coupled nuclei								
compd	1,2	2,3	3,4	4,5	5,6	5,6′	6,6′	1,3	2,4
α-GalNAc **6**	3.8	11.0	3.2	0.7	8.1	4.2	−11.7	0.4	0.4
	3.9	*10.3*	*3.4*	*1.2*	*8.2*	*4.2*	*−11.7*		
α-GlcNAc **7**	3.6	10.7	9.0	10.1	2.3	5.6	−12.3	0.3	0.5
	3.8	*9.8*	*9.2*	*10.0*	*2.3*	*5.6*	*−12.3*		
β-GlcNAc **8**	8.5	10.4	8.7	10.0	2.2	6.1	−12.3		0.6
	8.0	*9.5*	*9.2*	*10.0*	*2.3*	*6.2*	*−12.4*		
α-GulNAc **9**	4.1	3.7	3.9	1.2	8.2	4.3	−11.8	0.4	0.6
β-ManNAc **12**	1.5	4.5	9.8	10.0	2.3	5.3	−12.4		
	0.9	*3.2*	*9.6*	*9.7*	*2.4*	*6.5*	*−12.2*		
α-TalNAc **13**	1.2	5.0	3.2	1.5	8.0	4.1	−11.8	0.2	1.2
	∼1.9	*3.4*	∼3.5	∼1.3	*7.7*	*3.9*	*−11.2*		

[a] In ^2H_2O at 25 °C; in Hz (±0.1 Hz). Values in italics are for the corresponding methyl aldopyranosides (ref 44 for **6**−**8**; ref 10 for **12** and **13**).

TABLE 5. ^{13}C−^{1}H Spin-Coupling Constants[a] in Methyl 2-Acetamido-2-deoxy-D-[1-^{13}C]Aldohexopyranosides

	coupling constant (Hz)				
compd	$^1J_{C1,H1}$	$^2J_{C1,H2}$	$^3J_{C1,H3}$	$^3J_{C1,H5}$	$^3J_{C1,CH_3}$
α-GalNAc **6**	171.9	−2.5[b]	0.4	1.4	4.4
α-GlcNAc **7**	171.8	−2.7	0.7	1.4	4.4
	170.1	*+1.0*	br	*∼2.0*	*4.4*
β-GlcNAc **8**	161.8	−7.5	1.1	2.4	4.7
	161.3	*−6.3*	*1.2*	*2.3*	*4.6*
α-GulNAc **9**	171.0	−3.3	5.4	1.7	4.6
β-ManNAc **12**	162.2	−3.7	∼0	obs	4.6
	159.5	*±∼1.5*	*0*	*∼2.2*	*4.5*
α-TalNAc **13**	173.1	−2.7	0.1	1.8	4.4

[a] In ^2H_2O at 25 °C; in Hz (±0.1 Hz); br = broadened resonance; obs = obscured resonance. Values in italics are for the corresponding methyl aldopyranosides (ref 10). [b] $^2J_{C1,H2}$ signs determined from the expected shift to more negative couplings upon conversion of an OH to a $NHCOCH_3$ substituent at C2 (ref 37), DFT calculations (see Table 8), spectral simulation (see Figure S2, Supporting Information), and/or ^{1}H−^{1}H TOCSY cross-peak analysis (see Figure S3, Supporting Information).

$^1J_{C1,H1}$ in **7** and **8** differ slightly from $^1J_{C1,H1}$ in the corresponding reducing sugars (α-pyranose, 171.1 Hz; β-pyranose, 162.0 Hz) (Scheme 9). These changes may be caused, in part, by slightly different C1−O1 torsion angles for the OH and OCH_3 substituents at C1 (i.e., vicinal oxygen lone-pair effects on C−H bond length, modulated by the C1−O1 torsion angle, influence $^1J_{CH}$[35]).

$^3J_{C1,H3}$ and $^3J_{C1,H5}$ values in the aminosugars show the expected dependence on the C1−C2−C3−H3 and C1−O5−

(35) Serianni, A. S.; Wu, J.; Carmichael, I. *J. Am. Chem. Soc.* **1995**, *117*, 8645−8650.

SCHEME 9. *J*-Couplings in 22 and 23[a]

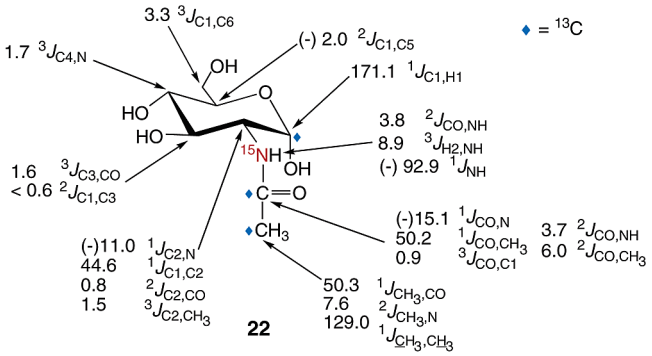

[a] Values in Hz; negative signs are indicated in parentheses.

C5−H5 dihedral angles, respectively (Table 5). Both couplings appear minimally affected by the change of substituent from OH to $NHCOCH_3$ at C2. Configuration at C1 appears to affect both couplings, with equatorial C1−O1 bonds slightly enhancing the coupling (e.g., $^3J_{C1,H3}$ and $^3J_{C1,H5}$ are slightly larger in **8** than in **6** and **7**) (Table 5). The presence of oxygen along the pathway also enhances the coupling (e.g., the average gauche $^3J_{C1,H5}$ is ~1 Hz larger than the average gauche $^3J_{C1,H3}$). The large $^3J_{C1,H3}$ for **9** reflects the ~180° torsion angle between the coupled nuclei (H3 is equatorial). These results track those observed previously in the methyl aldopyranosides.[10]

In contrast to $^3J_{C1,H3/H5}$, $^2J_{C1,H2}$ values change significantly when an $NHCOCH_3$ group replaces an OH group at C2. The available data indicate a shift to more negative values in the aminosugars, as confirmed via analysis of cross-peak displacements in representative ^{1}H−^{1}H TOCSY spectra (Figure S3, Supporting Information); absolute changes range from 1 to 4 Hz depending on ring configuration. Importantly, trends observed in these couplings are conserved in the aminosugars and the simple methyl aldohexopyranosides. For example, **8** exhibits a much different $^2J_{C1,H2}$ (−7.5 Hz) than the remaining compounds (−2.5 to −3.7 Hz), as is true for methyl β-D-glucopyranoside. This difference is predicted in the latter case by the projection rule proposed by Bock and Pedersen.[36]

Prior studies of nucleosides have suggested that a change from *O*- to *N*-substitution *at the coupled* carbon affects $^2J_{CCH}$ values much less than a similar change made at *the carbon bearing the coupled* proton.[37] $^2J_{CCH}$ values were reported to shift to more negative values in the latter case; the shift was estimated at ca. −2.5 Hz. Recent DFT calculations in 2-deoxy-β-D-ribofuranosylamine have shown that $^2J_{C2,H1}$ shifts to more negative values by ~3.5 Hz in the amine relative to that in the corresponding deoxyfuranose, in agreement with the nucleoside results.[31] The behavior of $^2J_{C1,H2}$ in **6**−**13** is consistent with these prior findings; for **7**, $^2J_{C1,H2}$ changes sign upon *N*-substitution, and for **12**, a similar sign change may occur.

$^1J_{C1,C2}$ values in **6**−**13** range from 42.5 to 46.9 Hz (Table 6). The change from *O*- to *N*-substitution at C2 reduces $^1J_{C1,C2}$ in aldopyranosyl rings by 1.7 ± 0.3 Hz based on data available for **7**, **8**, **11**, and **12**. These data support prior claims that $^1J_{CC}$ magnitude depends on the number and nature of electronegative substituents appended to the C−C fragment, with more electronegative substituents increasing the coupling.[38] $^1J_{CC}$ values also increase slightly upon methyl glycosidation. For example, $^1J_{C1,C2}$ in the α- (44.6 Hz) and β- (44.1 Hz) pyranose forms of *N*-acetyl-D-glucosamine (Scheme 9) are 0.3 and 1.0 Hz smaller, respectively, than related values in methyl glycosides **7** and **8**. Likewise, $^1J_{C1,C2}$ in the α- (46.2) and β- (46.1) pyranoses of D-glucose are 0.5 and 0.9 Hz smaller, respectively, than related values in their methyl glycosides. By comparison, $^1J_{C1,C2}$ in the α- and β-pyranose forms of D-glucosamine−HCl are 44.3 and 43.8 Hz, respectively.[39]

$^2J_{C1,C3}$ in **6**−**13** depends mainly on the orientation of OH substituents at the coupled carbons (Table 6). The di-equatorial orientation (**8**, **12**) gives the largest (most positive) coupling of ~4 Hz. The equatorial/axial arrangement (**6**, **7**, **10**, **11**, **13**) yields little or no coupling. Coupling is observed in the di-axial orientation (**9**), and based on the projection resultant rule,[40] it is expected to be negative ($^2J_{C1,C3}$ in α-D-allopyranose is −2.4 Hz).[40] $^2J_{C1,C3}$ appears minimally affected by a change in substitution at C2 from OH to $NHCOCH_3$.

Dual pathway $^{3+3}J_{C1,C4}$ values are rarely observed in aldopyranosyl rings. A small coupling (0.9 Hz) was observed in **9**; a similar coupling (0.7 Hz) has been reported in ethyl α-D-mannopyranoside.[3a]

Like $^2J_{C1,C3}$, $^2J_{C1,C5}$ depends on the orientation of OH substituents at the coupled carbons. In this case, however, only configuration at C1 is relevant. $^2J_{C1,C5}$ values in the α-pyranoses (**6**, **7**, **9**, **11**, **13**) range from −1.8 to −2.1 Hz and are negative in sign.[41] Little or no coupling is observed in β-pyranoses. Like $^2J_{C1,C3}$, $^2J_{C1,C5}$ appears to be minimally affected by a change of substitution at C2 from OH to $NHCOCH_3$.

$^3J_{C1,C6}$ depends mainly on the C1−O5−C5−C6 dihedral angle.[3a] In all cases examined, this angle is ~180°. Couplings in **6**−**13** range from 3.2 to 4.0 Hz, with larger values generally observed in the β-configuration. Other factors influence this coupling, however, notably the C5−C6 torsion angle, since an "in-plane" O6 enhances $^3J_{C1,C6}$ as does an "in-plane" O1.[3a] $^3J_{C1,C6}$ appears to be minimally affected by a change of substitution at C2 from OH to $NHCOCH_3$.

^{13}C−^{13}C couplings are also observed between C1 and the carbonyl carbon of the *N*-acetyl side-chain in **6**−**13** (Table 6). Couplings vary with ring configuration and range from ~0.6 to 2.2 Hz. These couplings are expected to depend on the

(36) Bock, K.; Pedersen, C. *Acta Chem. Scand.* **1977**, *B31*, 354−358.
(37) Bandyopadhyay, T.; Wu, J.; Stripe, W. A.; Carmichael, I.; Serianni, A. S. *J. Am. Chem. Soc.* **1997**, *119*, 1737−1744.
(38) Duker, J. M.; Serianni, A. S. *Carbohydr. Res.* **1993**, *249*, 281−303.
(39) Walker, T. E.; London, R. E.; Barker, R.; Matwiyoff, N. A. *Carbohydr. Res.* **1978**, *60*, 9−18.
(40) Church, T.; Serianni, A. S. *Carbohydr. Res.* **1996**, *280*, 177−186.
(41) Serianni, A. S.; Bondo, P. B.; Zajicek, J. *J. Magn. Reson.* **1996**, *112B*, 69−74.

TABLE 6. $^{13}C-^{13}C$ Spin-Coupling Constants[a] in Methyl 2-Acetamido-2-deoxy-D-[1-^{13}C]Aldohexopyranosides

	coupling constant (Hz)						
compd	$^1J_{C1,C2}$	$^2J_{C1,C3}$	$^{3+3}J_{C1,C4}$	$^2J_{C1,C5}$	$^3J_{C1,C6}$	$^2J_{C1,Me}$	$^3J_{C1,CO}$
α-GalNAc **6**	44.8	nc	nc	−2.1	3.4	−1.9	0.9
	46.0	*nc*	*nc*	*−1.9*	*3.6*		
α-GlcNAc **7**	44.9	nc	nc	−1.9	3.2	−1.9	nc
	46.2 (46.7)	*nc* (nc)	*nc* (nc)	*−1.8* (−2.0)	*3.3* (3.3)		
β-GlcNAc **8**	45.1	+4.4	nc	nc	4.0	−1.8	1.3
	46.0 (46.9)	*+4.5* (4.5)	*nc* (nc)	*nc* (nc)	*4.1* (4.1)		
α-GulNAc **9**	46.1	2.5[b]	0.9[b]	−1.8	3.1	−2.0	1.6
	45.9	*2.0*	*obs*	*−1.9*	*3.2*		
β-GulNAc **10**	46.9	nc	nc	nc	3.6	−2.0	2.2
	47.7	*nc*	*nc*	*nc*	*3.7*		
α-ManNAc **11**	45.3	nc	nc	−1.8	3.2	−∼1.7	obs
	46.7 (47.2)	*nc* (nc)	*nc* (0.7)	*−2.0* (−2.0)	*3.3* (3.2)		
β-ManNAc **12**	42.5	+4.0	nc	nc	4.0		
	42.7 (43.8)	*+4.0* (3.9)	*nc*	*nc*	*3.9* (4.0)		
α-TalNAc **13**	45.4	nc	nc	−1.9	3.2	−1.8	∼0.6
	46.5	*nc*	*nc*	*−1.8*	*3.3*		

[a] In Hz (±0.1 Hz); in ^2H_2O at 25 °C; nc denotes couplings <0.6 Hz; obs denotes obscured signal. Values in italics are for the corresponding aldohexopyranoses (refs 16 and 25). Values in parentheses are for the corresponding ethyl aldopyranosides (ref 3a). Indicated ^2J signs are predicted based on the projection resultant rule (ref 40) and experimental sign determinations in related systems (refs 41 and 45). [b] Assignments may be reversed.

TABLE 7. Computed $^1J_{CH}$ and $^1J_{CC}$ Values[a] in Compounds 14−21

	coupling constant (Hz)				
compd	$^1J_{C1,H1}$	$^1J_{C2,H2}$	$^1J_{C3,H3}$	$^1J_{C1,C2}$	$^1J_{C2,C3}$
α-Glc **14a**[d]	171.2 (170.1)[b]	150.2 (∼145.9)	143.0 (146.5)	45.5 (46.7)[c]	42.7 (38.2)[c]
α-Glc **14b**[e]	170.4	146.0	147.2	52.0	40.0
α-GlcNAc **15**	172.3 [171.8][h]	144.1	143.3	46.9 [44.9]	42.5 [36.7]
α-Man **16a**[f]	171.5 (171.0)	156.7 (148.5)	143.0	46.8 (47.2)[c]	41.6 (37.8)[c]
α-Man **16b**[g]	171.9	153.3	147.9	52.7	38.6
α-ManNAc **17**	172.3	149.4	145.2	48.7 [45.3]	41.0
β-Glc **18**	158.2 (161.3)	150.2 (145.0)	140.7 (142.9)	52.9 (46.9)[c]	40.4 (38.9)[c]
β-GlcNAc **19**	153.6 [161.8]	147.5	136.5	49.5 [45.1]	42.1 [37.0]
β-Man **20**	151.7 (159.5)	150.6 (147.9)	143.3 (142.0)	50.1 (43.8)[c]	38.8 (38.2)[c]
β-ManNAc **21**	158.2 [162.2]	148.3	139.1	45.6 [42.5]	42.7

[a] In Hz. [b] Values in parentheses are couplings observed experimentally in methyl pyranosides (ref 10). [c] Couplings observed in ethyl glycosides (ref 3a). [d] C1−C2−O2−O2H torsion, −47.0°. [e] C1−C2−O2−O2H torsion, −168.8°. [f] C1−C2−O2−O2H torsion, 43.3°. [g] C1−C2−O2−O2H torsion, 164.6°. [h] Experimental couplings in square brackets are from this study.

C1−C2−N2−CO torsion angle and thus may be useful in assessing side-chain conformation (see below).

E. DFT Calculations of *J*-Couplings. J_{CH} and J_{CC} values were calculated in model compounds **14**−**21** (Scheme 4; Scheme S1, Supporting Information) to further study the effect of OH vs $NHCOCH_3$ substitution at C2 on their magnitudes. Only the Fermi contact component was recovered; based on prior studies,[3a−c,24] the non-Fermi contact terms are expected to be negligible. All model glycosides lack hydroxyl groups at C4 and C6 to simplify the calculations, but their absence is not expected to significantly affect coupling pathways involving C1, C2, C3, and their attached protons. Only one C2−N2 torsion was examined in each structure, namely, that having H2 and the amide proton approximately trans. Also, only the trans configuration of the amide bond (carbonyl oxygen and amide proton trans) was considered (Scheme S1, Supporting Information).

Calculated $^1J_{CH}$ values were found to be very dependent on C−O torsion angles. For example, $^1J_{C1,H1}$ values of 171.2 and 170.4 Hz were calculated when the C1−C2−O2−H torsion angle is −47.0° (**14a**) and −168.8° (**14b**) (Schemes S1 and S2, Supporting Information), respectively (Table 7). Likewise, $^2J_{C2,H2}$ is 150.2 Hz in **14a** and 146.0 Hz in **14b**. Oxygen lone-pair effects on nearby bond lengths and angles are probably responsible for these effects. The smaller $^2J_{C2,H2}$ in **14b** is partly attributed to the presence of a vicinal O2 lone-pair anti to the C2−H2 bond, which lengthens the bond and reduces the coupling. 1,3-Lone-pair effects are also operating on $^1J_{C1,H1}$, as supported by the essentially identical computed $^1J_{C1,H1}$ in **16a** and **16b** (Schemes S1 and S2, Supporting Information) (no 1,3 effects are possible in the O1,O2-trans arrangement). In cases where experimental $^1J_{CH}$ couplings are available, their agreement with computed values is only moderate presumably because the experimental couplings reflect the presence of C−O populational averaging in solution. Notwithstanding the C−O torsional complications, computed $^1J_{C1,H1}$ generally decrease in the aminosugars, in agreement with the experimental findings. Computed $^1J_{C2,H2}$ and $^1J_{C3,H3}$ are smaller than $^1J_{C1,H1}$ in all compounds, also in agreement with experiment. These data show that predictions of absolute $^1J_{CH}$ in saccharides must take into account C−O torsional averaging as well as possible solvation effects.

$^1J_{C1,C2}$ is influenced by the C2−O2 torsion angle due to O2 lone-pair effects (Table 7). $^1J_{C1,C2}$ is considerably smaller in **14a** (45.5 Hz) than in **14b** (52.0 Hz) due to the presence of an O2 lone-pair anti to the C1−C2 bond. $^1J_{C2,C3}$ is predicted to be smaller than $^1J_{C1,C2}$, in agreement with experimental data, presumably due to the reduced number of electronegative substituents appended to the coupled carbons (two for $^1J_{C2,C3}$ vs three for $^1J_{C1,C2}$). $^1J_{CC}$ appears to decrease by 3−7 Hz for each loss of an oxygen substituent.[38] C−O torsional issues notwithstanding, $^1J_{C1,C2}$ appears to be slightly smaller in **15**,

TABLE 8. Computed $^2J_{CH}$ and $^2J_{CC}$ Values[a] in Compounds 14−21

	coupling constant (Hz)						
compd	$^2J_{C1,H2}$	$^2J_{C2,H1}$	$^2J_{C2,H3}$	$^2J_{C3,H2}$	$^2J_{C3,H4\ (ax)}$	$^2J_{C1,C3}$	$^2J_{C1,C5}$
α-Glc **14a**[d]	−0.5 (±1.0)[b]	−0.7 (−)	−4.4 (−)	−4.4 (−6.2)	−5.1 (−4.3)	−1.0 (nc)[c]	−2.2 (−2.0)[c]
α-Glc **14b**[e]	0.0	−1.3	−4.4	−3.3	−5.4	−0.9	−2.2
α-GlcNAc **15**	−2.0 [−2.7][h]	−0.1	−3.6	−5.7	−5.1	0.4 [nc]	−2.3 [−1.8]
α-Man **16a**[f]	−0.9 (−1.2)	−1.4 (∼−1.8)	1.5 (∼+1.4)	−3.1 (∼−3.7)	−5.2	0.7 (nc)[c]	−2.0 (−2.0)[c]
α-Man **16b**[g]	−0.2	−2.1	2.0	−1.9	−5.4	−0.8	−2.2
α-ManNAc **17**	−2.7	−0.7	0.6	−4.6	−5.1	0.3 [nc]	−2.1 [−1.8]
β-Glc **18**	−5.9 (−6.3)	0.4 (0)	−4.3 (−4.3)	−2.6 (−4.2)	−5.3 (−4.2)	3.9 (4.5)[c]	−0.7 (nc)[c]
β-GlcNAc **19**	−7.2 [−7.5]	1.4	−3.3	−5.5	−5.2	6.7 [4.4]	−0.6 [nc]
β-Man **20**	−0.5 (±1.5)	7.7 (+7.1)	2.5 (+1.5)	−2.4 (−4.6)	−5.5 (−5.3)	3.5 (3.9)[c]	−0.4 (nc)[c]
β-ManNAc **21**	−3.0 [−3.7]	6.4	1.5	−4.8	−5.2	6.0	−0.4

[a] In Hz. [b] Values in parentheses are couplings observed experimentally in methyl pyranosides (ref 10). [c] Couplings observed in ethyl glycosides (ref 3a); nc = no coupling was observed. [d] C1−C2−O2−O2H torsion, −47.0°. [e] C1−C2−O2−O2H torsion, −168.8°. [f] C1−C2−O2−O2H torsion, 43.3°. [g] C1−C2−O2−O2H torsion, 164.6°. [h] Experimental couplings in brackets from this study.

TABLE 9. Computed $^3J_{CH}$ and $^3J_{CC}$ Coupling Constants[a] in Compounds 14−21

	coupling constant (Hz)						
compd	$^3J_{C1,H3}$	$^3J_{C1,H5}$	$^3J_{C2,H4\ (ax)}$	$^3J_{C2,H4\ (eq)}$	$^3J_{C3,H1}$	$^3J_{C1,C6}$	$^3J_{C2,CH_3}$
α-Glc **14a**[d]	0.7 (br)[b]	1.6 (∼2.0)	2.2 (nc)[h]	7.4 (5.1)[c]	4.8 (5.2)	4.2 (3.3)	3.4
	[70°][i]	[−62°]	[−67°]	[176°]	[169°]	[−180°]	[−167°]
α-Glc **14b**[e]	1.4	1.5	2.3	7.4	5.1	4.1	3.7
	[65°]	[−61°]	[−67°]	[175°]	[173°]	[−179°]	[168°]
α-GlcNAc **15**	0.9 [0.7][j]	1.5 [1.4]	2.3	7.3	4.8	4.2 [3.2]	3.3
	[67°]	[−62°]	[−67°]	[176°]	[170°]	[−180°]	[−167°]
α-Man **16a**[f]	0.3 (nc)	1.5 (∼2.0)	1.9 (nc)	5.5	4.3 (4.6)	3.7 (3.2)	4.2
	[62°]	[−61°]	[−68°]	[175°]	[173°]	[−178°]	[−170°]
α-Man **16b**[g]	0.2	1.4	1.8	5.2	4.7	3.9	5.0
	[70°]	[−61°]	[−65°]	[176°]	[166°]	[−179°]	[−170°]
α-ManNAc **17**	0.2	1.6	1.7	5.3	4.3	3.8 [3.2]	4.7
	[66°]	[−60°]	[−69°]	[174°]	[171°]	[−178°]	[−170°]
β-Glc **18**	1.6 (1.2)	2.3 (2.3)	2.0 (nc)	7.2 (5.6)[c]	1.5 (1.1)	4.7 (4.1)	4.3
	[67°]	[−57°]	[−67°]	[175°]	[−65°]	[−175°]	[171°]
β-GlcNAc **19**	1.4 [1.1]	2.6 [2.4]	2.0	7.0	1.4	4.9 [4.0]	4.3
	[67°]	[−57°]	[−68°]	[175°]	[−64°]	[−175°]	[173°]
β-Man **20**	0.5 (nc)	2.3 (∼2.2)	1.6 (nc)	5.1	1.2 (nc)	4.7 (4.0)	4.4
	[67°]	[−59°]	[−66°]	[176°]	[−62°]	[−177°]	[173°]
β-ManNAc **21**	1.1 [nc]	2.5	1.8	5.4	1.1	4.6 [4.0]	4.2
	[63°]	[−58°]	[−69°]	[174°]	[−58°]	[−176°]	[173°]

[a] In Hz. [b] Values in parentheses are couplings observed experimentally in methyl or ethyl pyranosides (refs 3a and 10). [c] Couplings observed in methyl galactopyranosides (ref 44). [d] C1−C2−O2−O2H torsion, −47.0°. [e] C1−C2−O2−O2H torsion, −168.8°. [f] C1−C2−O2−O2H torsion, 43.3°. [g] C1−C2−O2−O2H torsion, 164.6°. [h] nc denotes no coupling (J < 0.6 Hz); br denotes broadened resonance. [i] Torsion angles in brackets were obtained from the DFT-optimized structures (see Schemes S1 and S2, Supporting Information). [j] Experimental couplings in brackets from this study.

17, **19**, and **21** relative to their respective methyl glycosides, in agreement with the experimental findings.

Computed $^2J_{CH}$ and $^2J_{CC}$ are generally in good agreement with experimental data (Table 8). The effect of C−O bond rotation on these two-bond couplings is smaller than observed for $^1J_{CH}$, and sign predictions appear robust. Computed $^2J_{C1,H2}$ shift to more negative values by 1.5−2.5 Hz when the C2 substituent is changed from OH to $NHCOCH_3$, in agreement with experimental findings. More significant differences between calculated and experimental $^2J_{CCH}$ are observed for $^2J_{C3,H2}$ (less negative in the calculations), presumably due to the lack of an O4 substituent in the model compounds, which can affect $^2J_{CCH}$ magnitudes via remote effects[10] and to C2−O2 torsional effects. The data suggest a shift to more negative $^2J_{C3,H2}$ in the aminosugars, analogous to observations for $^2J_{C1,H2}$. Computed $^2J_{C3,H4}$ are more negative than corresponding experimental values, again presumably due to the lack of an OH group on the carbon bearing the coupled proton. These couplings appear unaffected by substituent structure at C2.

Small $^2J_{C1,C3}$ values are computed in α-pyranosides **14**−**17** (+0.7 to −1.0 Hz), and large values are computed in β-pyranosides **18**−**21** (+3.5 to +6.7 Hz), in general agreement with experiment. A significant deviation between computed and experimental $^2J_{C1,C3}$ values was found in **19**, for reasons that are unknown. In contrast to $^2J_{C1,C3}$, $^2J_{C1,H5}$ is larger in **14**−**17** (ca. −2.1 Hz) than in **18**−**21** (ca. −0.5 Hz), in good agreement with experiment. These two-bond couplings appear unaffected by C2−O2 torsion and by C2 substituent structure.

Computed $^3J_{C1,H3}$ and $^3J_{C1,H5}$ are in good agreement with experimental data (Table 9) for *gluco* and *manno* configurations. Interestingly, $^3J_{C1,H3}$ appears on average to be slightly larger in β-pyranosides **18**−**21** than in α-pyranosides **14**−**17**, although the difference is small and the effects of C−O torsions cannot be completely excluded. Likewise, $^3J_{C1,H5}$ appears larger in the β-pyranosides; in this case, the conclusion is less ambiguous since C−O torsions affect this pathway minimally. Similar observations have been reported based on trends observed in experimental $^3J_{C1,H3}$ and $^3J_{C1,H5}$.[10] Gauche $^3J_{C1,H5}$ are predicted to be larger than gauche $^3J_{C1,H3}$, again in agreement with experiment.[10] The computed couplings between C2 and $H4_{ax/eq}$ deviate from experimental findings due to the lack of an O4 substituent in the model structures. Interestingly, the relatively wide range of anti couplings observed for $^3J_{C2,H4(eq)}$ suggest that O2/N2 orientation influences this coupling in a manner analo-

gous to $^3J_{C1,H3}$, with an in-plane O2/N2 increasing the coupling. $^3J_{C3,H1}$ is larger in **14**−**17** than in **18**−**21** due to the significantly different C3−C2−C1−H1 dihedral angles (∼60° vs ∼180°).

$^3J_{C1,C6}$ shows a dependence on anomeric configuration, with an "in-plane" O1 enhancing the coupling.[3a] For example, $^3J_{C1,C6}$ is smaller in **14**/**15** than in **18**/**19**, and $^3J_{C1,C6}$ is smaller in **16**/**17** than in **20**/**21**. Absolute values of the computed couplings are larger than the experimental values presumably because of the lack of O6 in the model compounds.

F. Side-Chain ^{13}C/^{15}N Labeling of 2-Aminosugars. 2-Acetamido-2-deoxy-D-glucose was prepared with ^{13}C-labeling at C1 and both acetyl carbons, and with ^{15}N-labeling (Figure S4, Supporting Information). Analysis of the ^{13}C NMR spectrum revealed multiple J_{CC} and J_{CN} couplings within the α- (**22**) and β- (**23**) pyranoses which are summarized in Scheme 9.

Intra-ring ^{13}C−^{13}C couplings involving C1 include $^1J_{C1,C2}$, $^2J_{C1,C3}$, $^2J_{C1,C5}$, and $^3J_{C1,C6}$. Most of these couplings are comparable in magnitude (±0.1 Hz) to those observed in the methyl glycosides **7** and **8** (Table 6). The exception is $^1J_{C1,C2}$, which differs by 0.3 Hz between **7** and **22**, and by 1 Hz between **8** and **23**. This trend is observed in other reducing sugar/methyl glycoside comparisons (data not shown). In general, methyl glycosidation increases $^1J_{C1,C2}$ by 0.3−0.4 Hz in α-aldopyranosyl rings and by 0.9−1.0 Hz in β-aldopyranosyl rings. In contrast, $^1J_{C1,H1}$ increases by ∼0.7 Hz upon methyl glycosidation of **22**, whereas $^1J_{C1,H1}$ decreases slightly (0.2 Hz) upon methyl glycosidation of **23**. A small change (0.3 Hz) is also observed in $^3J_{C1,C6}$ between **8** and **23**.

Numerous *J*-couplings were observed within the *N*-acetyl side-chain (Figure S4, Supporting Information). These include the vicinal couplings $^3J_{C1,CO}$, $^3J_{C3,CO}$, $^3J_{C1,NH}$, $^3J_{C3,NH}$, and $^3J_{H2,NH}$, all of which presumably report on the torsional preferences of the C2−N2 bond, although Karplus curves for these pathways remain to be formulated. Vicinal coupling between C2 and the side-chain methyl group was also observed in **22** and **23** (∼1.5 Hz), but it is unclear how this *J*-coupling may be influenced by the cis−trans configuration of the amide bond.

Vicinal coupling of the ^{15}N to C4 (∼180° dihedral angle) was observed in both anomers (1.5−1.7 Hz; sign unknown). There is no apparent $^2J_{NC}$ involving C1 and C3 in **22** and **23**. A $^2J_{NC}$ is, however, observed for the methyl carbon of the side-chain (7.6−7.8 Hz; sign unknown). $^1J_{C2,N}$ (ca. −11 Hz) and $^1J_{CO,N}$ (ca. −15 Hz) are comparable in magnitude and probably negative in sign.[42] $^1J_{NH}$ appears to differ in **22** (−92.9 Hz) and **23** (−91.7 Hz). A number of geminal couplings were also observed (e.g., $^2J_{CO,NH}$, $^2J_{CH3,N}$, $^2J_{C2,CO}$), but their dependencies on side-chain structure/conformation are presently unknown.

Taken collectively, the ensemble of *J*-couplings involving *N*-acetyl side-chain atoms should provide useful, redundant information about the torsional preferences of the C2−N2 bond, and possibly about the cis−trans equilibrium of the amide bond. At present, the preferred H2−C2−N2−H torsion in structures such as **22** and **23** is generally believed to be trans,[43] while amide configuration is assumed to be trans. However, relative configuration at C1, C2, and C3 may modulate one or both of these preferences.

TABLE 10. Structure−Spin Coupling Correlations in 2-Acetamido Sugars

J-coupling	structural correlations
$^3J_{H2,H3}$	increases in C2−NAc derivatives (0.9−1.6 Hz)[a]
$^1J_{C1,H1}$	increases in C2−NAc derivatives (0.5−2.7 Hz)[a]
$^1J_{C1,C2}$	decreases in C2−NAc derivatives (∼1.7 Hz)[a]
$^2J_{C1,H2}$	shifts to more negative (−) values in C2−NAc derivatives (1−4 Hz)[a]
$^3J_{C1,H5}$, $^3J_{C1,H3}$, $^2J_{C1,C3}$, $^3J_{C1,C6}$	shifted to more positive (+) values when "in-plane" terminal oxygen(s) are present in the pathway

[a] Relative to methyl aldopyranosides.

Conclusions

A simple and general chemical route to prepare 2-amino-2-deoxy-D-aldohexoses has been developed that is applicable to ^{13}C, ^{2}H, and/or ^{15}N labeling with use of inexpensive and readily available labeled precursors. Simple D-aldopentosylamines can be prepared in good yield, are chemically stable, and convert rapidly to 2-amino-2-deoxyaldononitriles, which are subsequently reduced catalytically to give C2-epimeric 2-amino-2-deoxyaldohexoses. Solution conditions were determined to minimize pentosylamine hydrolysis during cyanide addition, and separation of the epimeric amines can be achieved either as their free amines or their *N*-acetylated derivatives. This simple methodology provides access to the biologically relevant GlcNAc and GalNAc structures, but importantly to other ring configurations that may be valuable in studies of biological structure−function properties.

^{13}C and ^{1}H NMR data were obtained on the D-aldopentosylamines in aqueous solution at pD 10.5. At this pD, hydrolysis is slow, and well-resolved spectra are obtained. Solution studies suggest that orientation of the C1−N1 bond plays a dominant role in dictating both preferred anomeric configuration and ring conformation in these structures, with an equatorial orientation preferred in all cases. Time-lapse ^{13}C NMR studies of the hydrolysis of ^{13}C-labeled β-D-xylopyranosylamines revealed four major intermediates that were assigned to the two anomeric D-xylofuranosylamines, α-D-xylopyranosylamine, and an acyclic carbinolamine. Conformational preferences of xylofuranosylamines appear to differ significantly from those of simple xylofuranoses based on $^3J_{H1,H2}$ analyses, indicating that substitution of NH_2 for OH at C1 significantly changes preferred furanose ring conformation.

Fischer glycosidation of the free HexNAc sugars was rapid and yielded pure methyl glycosides after column purification. Access to pure glycoside anomers simplified subsequent NMR analyses by reducing the spectral complexity inherent to reducing sugars. *N*-Acetyl substitution at C2 caused minimal change in intra-ring J_{CH} and J_{CC} values in most cases, and thus prior empirical rules governing the effect of pyranosyl ring structure on *J*-coupling magnitude and sign based on observations in simple aldohexopyranosyl rings appear applicable to the 2-acetamido-2-deoxy ring system. There are, however, some exceptions, specifically for $^1J_{C1,C2}$, $^1J_{C1,H1}$, and $^2J_{C1,H2}$ (Table 10). For $^2J_{C1,H2}$, *O*- to *N*-substitution at C2 consistently shifts these couplings to more negative values. Overall, these results are important for anticipated NMR studies of GlcNAc- and GalNAc-containing oligosaccharides. A key question that remains unanswered is how long-range J_{CC} values involving

(42) (a) Levitt, M. H. *Spin Dynamics. Basics of Nuclear Magnetic Resonance*; John Wiley & Sons: New York, 2001; p 419. (b) Ando, I.; Webb, G. A. *Theory of NMR Parameters*; Academic Press: New York, 1983; pp 83−113.

(43) (a) Cowman, M. K.; Cozart, D.; Nakanishi, K.; Balazs, E. A. *Arch. Biochem. Biophys*. **1984**, *230*, 203-212. (b) Holmbeck, S. M. A.; Petillo, P. A.; Lerner, L. E. *Biochemistry* **1994**, *33*, 14246−14255. (c) Scott, J. E.; Heatley, F. *Proc. Natl. Acad. Sci.* **1999**, *96*, 4850−4855.

C2 as the coupled carbon are affected by *N*-substitution at C2. This question is particularly relevant for trans-glycoside $^3J_{C2,Cx}$, which are useful structural constraints for the ϕ torsion angle in *O*-glycosidic linkages.[3a] This problem is currently under investigation.

DFT studies showed that $^1J_{CH}$ and $^1J_{CC}$ are significantly affected by exocyclic C−O torsions, whereas $^3J_{CH}$ and $^3J_{CC}$ appear much less influenced by them. This observation suggests that efforts to interpret the former *J*-couplings in solution will need to take into account the averaging of exocyclic C−O rotamer populations and possibly other factors.

Exocyclic *N*-acetyl side-chain conformation in 2-acetamido-2-deoxyaldohexoses has been implicated in determining their biological properties, most notably in heteropolysaccharides such as hyaluronic acid.[43] ^{13}C- and ^{15}N-labeling of this side-chain makes available a large ensemble of scalar couplings that are sensitive to the C2−N2 torsion angle, to amide bond configuration, and/or to other presently unrecognized structural features. Prior studies have utilized only one of these couplings, $^3J_{H2,NH}$, to evaluate C2−N2 torsional preferences.[43] As shown in recent studies of exocyclic hydroxymethyl (CH_2OH) conformation,[44] the use of multiple, redundant *J*-couplings sensitive to the same conformational domain can significantly improve determinations of rotamer populations in solution. In the exocyclic *N*-acetyl case, at least two additional *J*-couplings, $^3J_{C1,CO}$ and $^3J_{C3,CO}$, are likely to depend on the C2−N2 torsion angle, and thus their parametrization should prove useful in this context. Likewise, while it is generally assumed that amide bond configuration in 2-acetamido-2-deoxy-D-aldohexoses is trans, it is not unreasonable to expect the presence of some cis configuration in solution, albeit in minor amounts. Further studies of chemical shifts and/or *J*-couplings within the *N*-acetyl side-chain may shed further light on this question.

Acknowledgment. This work was supported by grants from the National Institutes of Health (GM) (to A.S.). The Notre Dame Radiation Laboratory is supported by the Office of Basic Energy Sciences of the United States Department of Energy. This is Document No. NDRL-4607 from the Notre Dame Radiation Laboratory.

Supporting Information Available: Table S1 showing HRMS data obtained on aldopentosylamines **2**−**5**; Table S2 showing HPLC retention times of aminosugars; Scheme S1 showing DFT-computed molecular structures of **14a**, **15**, **16a**, and **17**−**21**; Scheme S2 showing DFT-computed molecular structures of **14** and **16**; Figure S1 showing MS data for **7**; Figure S2 showing real and simulated 600-MHz ^{1}H NMR spectra of **7**; Figure S3 showing the assignment of the negative sign of $^2J_{C1,H2}$ in **7** from ^{1}H−^{1}H TOCSY data; Figure S4 showing partial ^{13}C NMR spectra of **22** and **23**; Cartesian coordinates for DFT structures **14**−**21**; ^{13}C{^{1}H} NMR spectra (150 MHz) of **2**−**5**; and ^{1}H NMR spectra (600 MHz) of **2**−**5**. This material is available free of charge via the Internet at http://pubs.acs.org.

JO051510K

(44) Thibaudeau, C.; Stenutz, R.; Hertz, B.; Klepach, T.; Zhao, S.; Wu, Q.; Carmichael, I.; Serianni, A. S. *J. Am. Chem. Soc.* **2004**, *126*, 15668−15685.

(45) Zhao, S.; Bondo, G.; Zajicek, J.; Serianni, A. S. *Carbohydr. Res.* **1998**, *309*, 145−152.